solids

MDPI

Review

Two-Dimensional Quantum Dots: From Photoluminescence to Biomedical Applications

Mariana C. F. Costa [1,2,3,*], Sergio G. Echeverrigaray [2], Daria V. Andreeva [1,2,3], Kostya S. Novoselov [1,2,3] and Antonio H. Castro Neto [1,2,3,*]

[1] Department of Materials Science and Engineering, College of Design and Engineering, National University of Singapore (NUS), Singapore 117575, Singapore
[2] Centre for Advanced 2D Materials (CA2DM), National University of Singapore (NUS), Singapore 117546, Singapore
[3] Institute for Functional Intelligent Materials (I-FIM), National University of Singapore (NUS), Singapore 117544, Singapore
* Correspondence: mariana.cfcosta@u.nus.edu (M.C.F.C.); c2dhead@nus.edu.sg (A.H.C.N.)

Abstract: Quantum dots (QDs) play a fundamental role in nanotechnology because of their unique optical properties, especially photoluminescence (PL). Quantum confinement effects combined with tailor-made materials make QDs extremely versatile for understanding basic physical phenomena intrinsic to them as well as defining their use in a vast range of applications. With the advent of graphene in 2004, and the discovery of numerous other two-dimensional (2D) materials subsequently, it became possible to develop novel 2D quantum dots (2DQDs). Intensive research of the properties of 2DQDs over the last decade have revealed their outstanding properties and grabbed the attention of researchers from different fields: from photonics and electronics to catalysis and medicine. In this review, we explore several aspects of 2DQDs from their synthesis, functionalization, and characterization to applications, focusing on their bioimaging, biosensing, and theranostic solutions

Keywords: 2D materials; quantum dots; synthesis; functionalization; characterization; fluorescence properties; bioimaging; biosensing; theranostic applications

Citation: Costa, M.C.F.; Echeverrigaray, S.G.; Andreeva, D.V.; Novoselov, K.S.; Neto, A.H.C. Two-Dimensional Quantum Dots: From Photoluminescence to Biomedical Applications. *Solids* **2022**, *3*, 578–602. https://doi.org/10.3390/solids3040037

Academic Editors: Mohammed Jaouad Meziani, Antonio Polimeni and Zhaohui Li

Received: 15 September 2022
Accepted: 12 October 2022
Published: 19 October 2022

1. Introduction to 2D Quantum Dots

Quantum dots (QDs) are synthetic nanoparticles—in the range of 2 nm to 10 nm, of crystalline materials in which their size dimensions influence the quantum confinement of electrons and holes [1]. Although QDs were first theorized in 1970's, they have been only experimentally demonstrated in the 1980's [2,3]. Semiconductor QDs are defined as nanoparticles with spherical shape and crystalline core/shell structures, combining elements from groups II–VI of the periodic table (CdSe, CdTe, CdS, PbSe, ZnS and ZnSe) or III–V (GaAs, GaN, InP and InAs), and coated with an outer shell layer of ZnS or CdS to prevent toxicity [4]. In a typical QD, the core emission is weak and relatively unstable, whereas the shell is practically non-reactive and insulates the core. Organic molecules can be covalently bonded to the shell, enabling conjugation of species (such as antibodies, nucleic acids) to a hydrophilic QD [5]. Figure 1 shows a schematic representation of a QD with core/shell structure and organic ligands attached.

Overall, colloidal QDs are classified into different categories, such as (i) core-type QDs, defined as single component materials, such as chalcogenides (selenides, sulphides, or tellurides) of metals (cadmium, lead or zinc), forming CdS, PbS, CdTe, CdSe, MoS_2, among others; (ii) core-shell QDs, made of two components and an external shell that allows to improve the quantum yield and stability of nanocrystals (e.g., CdSe/ZnS). To further enhance their efficiency, avoid photobleaching, or leaking of semiconductor nanocrystals, an additional shell of semiconducting material is grown around QDs; (iii) alloyed QDs: multicomponent materials with gradient internal structures (e.g., CdS_xSe_{1-x}/ZnS) used to

tune the electronic and optical properties, but preserving the crystallite size [6,7]. Several synthesis routes allow to obtain these artificial nanocrystals in mass scale with controlled size, shape, composition, structures, and unique physical and chemical properties. Of particular interest are their optical properties, such as photo- and electro-luminescence, that allow fine tuning of the spectral selectivity of such objects, as well as amphiphilic nature, and colloidal properties. Currently, QDs have been popularly used for light-emitting diodes (LEDs) [8], displays [9], photovoltaic cells [10,11], transistors [12,13], quantum computing [14], bioimaging [15,16], biosensing [17,18], among others.

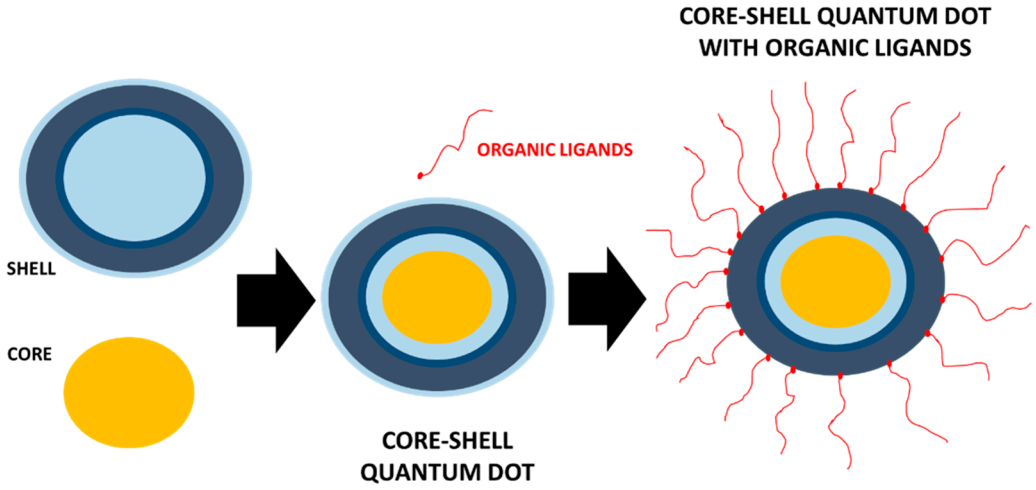

Figure 1. Schematic illustration of a shell-core quantum dot (QD) with organic ligands covalently attached to the shell.

The field of two dimensional (2D) materials has developed significantly over the past two decades and achieved certain levels of maturity in terms of scientific accomplishments and technological advances for industrial applications. The electronic and optical response of 2DQDs arise from the quantum effects that play an important role in their physical properties [19]. Among the main advantages of 2DQDs are highly tunable photoluminescence (PL) effect, enhanced photostability, atomically-thin structure, molecular size, biocompatibility, and easy functionalization [20,21]. Because of their small dimensions, QDs lead to quantization of energy levels according to the laws of quantum mechanics. 2DQDs can be thought as quantum wells that geometrically confine electrons, as it can be seen in Figure 2a. Hence, the size of 2DQDs directly influences the optical properties, ensuring that only specific wavelengths of light can be either emitted or absorbed.

Especially interesting are the photoluminescence (PL) properties of 2DQDs, schematically illustrated in Figure 2b. Specifically, this phenomenon can be understood in terms of having an electron in a low energy state that is excited to a higher electronic excited state leaving a hole behind. Such excited electron can interact with atoms in the material, emit and absorb phonons (resulting in atomic vibrations) and/or recombine with its counterpart left-over hole, leading to photon emission [22]. The PL effect will be further discussed below.

As the properties of QDs, regardless their dimensionality, are governed by the laws of quantum mechanics, in the simplest approximation, they can be though as an empty box of volume $L_x \times L_y \times L_z$ in each correspondent direction (x, y, z), and impenetrable walls. An electron inside of such box is described by a wave-function Ψ (x, y, z), obeying the Schrödinger equation [23]. To solve this elementary problem, one can use the Schrödinger equation and calculate the energy of an electron, E, inside of the box:

$$\mathrm{E}(\mathrm{n}_x,\ \mathrm{n}_y, \mathrm{n}_z) = \frac{\hbar^2 \pi^2}{2m_e}\left[\left(\frac{n_x}{L_x}\right)^2 + \left(\frac{n_y}{L_y}\right)^2 + \left(\frac{n_z}{L_z}\right)^2\right] \quad (1)$$

where m_e is the electron mass, (n_x, n_y, n_z) are the three non-zero integers $(n_x, n_y, n_z = 1, 2, 3, 4 \ldots)$ and $\hbar$ is the reduced Planck constant. The dimensionality only enters through the size of the box $L_x \times L_y \times L_z$. Each set of integers (n_x, n_y, n_z) represents a quantum state that, according to the Pauli exclusion principle, can be occupied only by 2 electrons (one spin up and another spin down). At zero temperature, the states are occupied starting from the lowest energy states, that is, with the smallest integers ($n_x = 1$, $n_y = 1$, $n_z = 1$), until a final number of electrons, N_e, occupies the QDs. The highest energy occupied state of the QDs, has a maximum energy, E_F, the so-called Fermi energy [23].

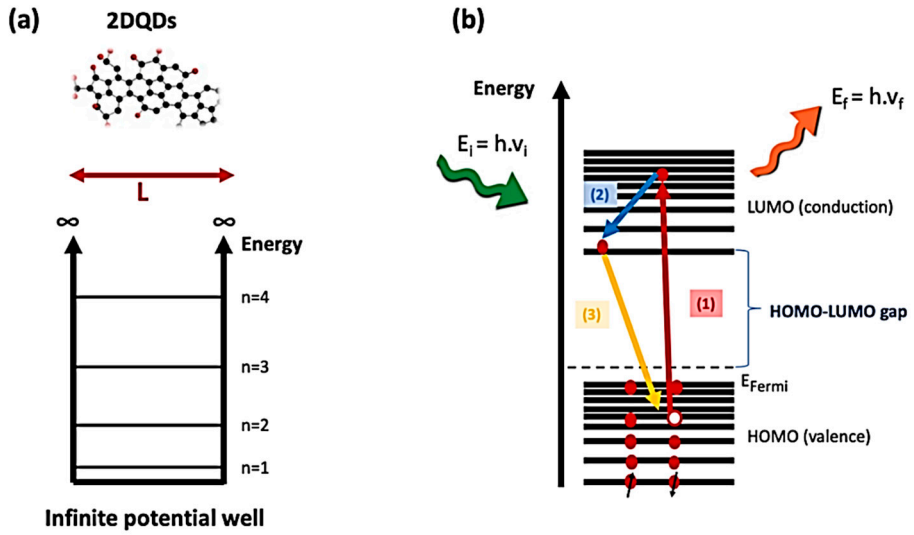

Figure 2. Schematic illustration of the PL mechanism. (**a**) A 2DQD with length L and an infinite quantum well with quantized energy states. (**b**) Representation of the PL effect that occurs in three different stages: (**1**) absorption of light; (**2**) non-radiative transitions due to phonon emission and absorption; (**3**) electron-hole recombination and emission of light.

A three dimensional quantum dot (3DQD) can be seen as a box, where L_x, L_y and L_z have similar size, say, a few nm. In this context, a 2DQD can be seen as a special case of 3DQD, where L_x and L_y have similar size (a few nm), but L_z is much smaller, say, of the order of atomic dimensions (a few angstroms) [24,25]. Note that, from Equation (1), for a given state, that is, for a fixed set of integers (n_x, n_y, n_z), the energy grows as $1/L^2_{x,y,z_x}$ as the size of the box is reduced. According to Equation (1), if L_z is reduced to atomic size, the energy of the states with $n_z > 1$ "float upwards" in energy. This means that the energy states become so large that, eventually, they surpass the E_F and cannot be occupied anymore. In this limit, only states of $n_z = 1$ are occupied and the 3DQD becomes a 2DQD.

Graphene is the world's first 2D material and has unique properties, such as high electrical and thermal conductivities, high optical activities, large surface area, ultrafast carrier mobility, flexibility, lightness, mechanical stability, and tuneable chemical functionality. In particular, for graphene-based micrometre-sized devices, the zero band gap and low electromagnetic absorptivity make the use of this material in optoelectronic devices less than optimal [26–28]. Alternatively, synthesized nm-sized graphene quantum dots (GQDs) are highly stable and conductive with a unique fluorescence resultant from the modification of its electronic states due to their dimensions.

GQDs have interesting characteristics such as PL, low toxicity, high chemical and photostability against bleaching and blinking, biocompatibility and high solubility. These properties make GQDs extremely attractive for a large number of promising applications in bioimaging, biosensing, optoelectronics, photovoltaics, and energy storage and energy conversion devices [22,29–32]. Beyond graphene [15,33–36], there have been great efforts dedicated to exploration of other materials for 2DQDs, such as graphene oxide [37,38] transition metal dichalcogenides (TMD) [39], phosphorene and MXenes [29], hexagonal

boron nitride (hBN) [40], apart from other thousands of crystals with nano and sub-nano thickness. Currently, 2DQDs have become a cutting-edge research topic and have great appeal to several industrial sectors, however there are limitations for real life applications mainly related to the potential risks of quantum dots in the biomedical field [20]. Apart from biomedical applications, QDs have been used commercially in several products and the levels of exposure of them to humans, animals, and plants had significantly increased over the past decades.

There have been experimental and theoretical researches on understanding not only the toxicity of quantum dots to the human body through in vivo and in vitro analyses, but also simulating the interactions of DNA molecules with functional groups attached to 2DQDs [7,41–46]. Such studies are of paramount importance to clarify what are the long-term consequences of such small-size nanoparticles on biological systems. In fact, the size of 2DQDs interconnects their intrinsic features (such as photoluminescence properties) to the quantum confinement and optical properties advantages, making them promising candidates for imaging, sensing, tracking, and real-time monitoring of diseases [47,48]. More recently, a research group developed an ultrasensitive and nucleic amplification-free electrochemical biosensor based on BN-QDs capable to detect and diagnose SARS-CoV-2. Such biosensors have been shown as potential candidates for accurate, sensitive and timely diagnosis for clinical analysis with results recognition as short as 30 min of incubation time [49].

Generally, there are two types of approaches to produce 2DQDs: (i) top-down methods, in which a macroscopic layered 3D crystal is exfoliated and broken down to 2DQDs; (ii) bottom-up methods, in which 2DQDs are chemically grown from properly chosen molecules under suitable conditions [34,50–52]. The particle size, edge type, bandgap extension, presence or absence of functionalization, are important characteristics of QDs that can be tailored by choosing different strategies according to the desired properties and applications [53]. It has been demonstrated that the PL property of 2DQDs is one of the most fascinating characteristics of these nanomaterials. Also, several microscopy and spectroscopy techniques have been used to characterize different types of 2DQDs, assisting researchers in researching of the optical and electronic characteristics of such objects. In this review, we summarize recent studies on the synthesis and functionalization of 2DQDs, their PL properties, and the main characterization techniques used for these systems. Finally, we discuss the advances in the applications of such quantum systems.

2. Synthesis of 2D Quantum Dots

The methods for synthesizing nanomaterials can be classified into two main categories: top-down and bottom-up approaches (see Figure 3). The former is done via either physical or chemical interactions to reduce a bulk layered 3D crystal into smaller structures. Some popular top-down techniques to produce 2D materials are the micromechanical and the liquid-phase exfoliation processes [54–56], for which non-uniform 2DQDs are produced due to a large distribution of sizes and morphologies obtained. The latter is achieved through the use of molecular and/or atomic precursors as starting materials, allowing to get greater control over QD's morphologies. The synthesis via chemical vapor deposition (CVD), thermal decomposition of small molecules, and epitaxial grown on monocrystalline substrates are a few examples of bottom-up methods [34,50–52]. These synthetic routes are used for production of most of the 2DQDs with tunable size, controlled edge structures, or even for doping or functionalization of such materials, leading to potentially large-scale productions [22]. Herein, for a better understanding, each technique is discussed separately.

2.1. Top-Down Approaches

In a top-down approach, bulk layered 3D materials are exposed to extreme conditions, such as relatively concentrated acids, oxidizing agents or high temperature, to produce 2DQDs. Since such aggressive conditions are required, it is extremely challenging to control

the QDs morphology and size distributions [22,57]. Several top-down routes have been developed and a few are listed below.

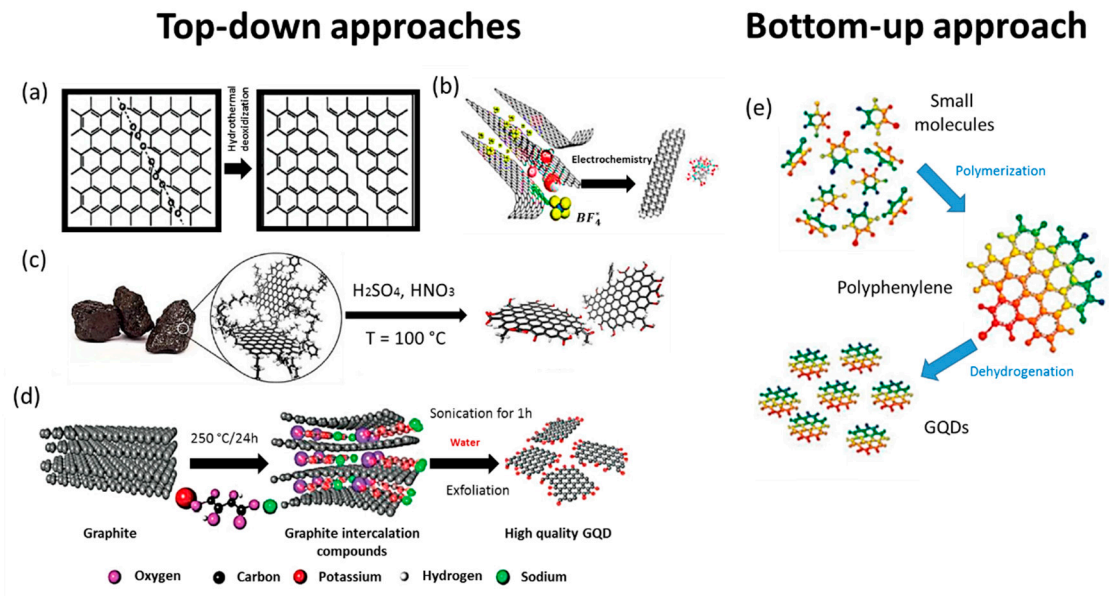

Figure 3. Fabrication of GQDs by top-down approaches: (**a**) hydrothermal deoxidization; (**b**) electrochemical exfoliation; (**c**) acid etching; (**d**) ultrasonic exfoliation; and a bottom-up approach: (**e**) carbonization route. Reprinted with permission [29].

2.1.1. Hydrothermal or Solvo-Thermal

Hydrothermal process is a popular wet chemistry method that allows to produce complex materials with high crystallinity of an aqueous solution in a high temperature—high pressure reaction environment. Overall, it is considered a low cost, eco-friendly and nontoxic technique to synthesize high quality 2DQDs made of graphene and reduced graphene oxide (rGO) [33,48,49], molybdenum disulphide (MoS_2) and tungsten disulphide (WS_2) [12,50]. Briefly, bulk 3D layered precursor materials are lacerated into small pieces due to the breakdown of van der Waals and covalent bonds, converting the raw materials into products [16,48].

2.1.2. Electrochemical Exfoliation with Ion Intercalation

The electrochemical cleavage of materials, such as carbon nanotubes, graphite rods, graphene films and CVD-grown graphene generates a high yield of GQDs. In electrochemical exfoliation, the hydroxyl and oxygen radicals from oxidation of water actuate as "scissors" at the edges and defect sites of the material to produce quantum dots [58]. This strategy is of great interest for production of pure materials since does not require the use of chemical oxidants as the driving force for intercalation/exfoliation. The relatively large interlayer distance between sheets of TMD materials is advantageous for obtaining large scale production of 2DQDs. By intercalating lithium (Li) and potassium (K) ions into the bulk structure, exfoliation is promoted, and the lateral dimensions of TMDs are reduced, providing TMD-QDs of the order of 2–5 nm [59]. In addition, it has also been shown that mass production of MoS_2 QDs is viable via variable electrochemical methods [60,61].

2.1.3. Acid Etching

In this approach, bulk carbon-based precursors, such as carbon fibers, carbon nanotubes, graphene oxide, carbon black, among others are treated using strong acids, such as nitric acid (HNO_3), in which the negatively charged oxygenated groups make the surface of materials hydrophilic, and some defect sites are boosted. As a result, large-scale production of GQDs is possible using acid etching with improved performance [57,62].

2.1.4. Ultra-Sonication

This is a cost-effective and environmental-friendly route to reduce the lateral size dimensions of precursors by using mechanical forces. The approach takes advantage of the weak van der Waals interactions between stacked layers of 2D materials, such as MoS_2, WS_2, black phosphorous (BP), and graphene, leading to the formation of quantum dots based on these materials [20,40,63]. Some purification steps and thermal processes are used to cleave 2D structures by ultrasonic treatment in order to produce nanometer-sized structures at room temperature [37].

2.1.5. Electro-Fenton

Electrochemically induced Fenton (electro-Fenton) reaction has been shown as an attractive method to produce 2DQDs due to its high effectiveness, fast treatment rate, and environmentally compatibility. In electro-Fenton process of graphene oxide, hydrogen peroxide (H_2O_2) is generated in situ at the cathode, and ferrous ions are added to the system in order to enhance the oxidation activity and form hydroxyl radicals. The ferrous ions (Fe^{2+}) regenerate at the cathode, and further produce additional hydroxyl radicals in the electrochemical mode. Since graphene and GO sheets are aromatic structures, they easily react with hydroxyl radicals, breaking the nanosheets apart and transforming them into GQDs with great photoluminescence properties. Following the same electrochemical procedures and using pre-Fenton reagents (O_2 and Fe^{2+}), it has been also shown that MoS_2 nanosheets could react with hydroxyl radicals and form MoS_2-QDs with nanoporous facets by electro-Fenton reactions on a mass scale. For this high yield approach, the reaction time determines the effect of the presence of radical groups [64].

2.2. Bottom-Up Approaches

In contrast to the top-down approaches, the bottom-up routes of 2DQDs are based on small organic or inorganic precursors, such as reactive atoms and molecules that produce more complex structures. Because they are versatile and highly customizable, they provide greater control of structural dimensions and morphologies, and consequent articulation of specific properties of the products. Thus, surface modification or doping during syntheses offer well-defined molecular size, shape and properties to higher performance 2DQDs, with high-yield and low cost mass production [65,66]. The limiting factor is associated with the formation of relatively small size 2DQDs compared to the top-down counterparts.

2.2.1. Template Synthesis

Template-assisted synthesis includes the oriented growth of materials on the top of specific substrates. The template is usually removed through high temperature or pH adjustments, leaving only the 2DQDs by-products copying the template design. It has been shown that the intermolecular carbonization of 1,3,4-Tri-amino-2,4,6-trinitrobenzene (TATB) favors the formation of small and controlled-sized nitrogen-doped GQDs in a soft-template synthesis approach [67]. Another group demonstrated the production of large photoluminescent disk-like GQDs by using hexa-peri-hexabenzocoronene (HBC), a polycyclic aromatic hydrocarbon (PAHs) as a precursor. TATB and HBC are aromatic molecules with a tendency to form graphitic-like multilayered structures after thermal processes that are commonly used as precursors as well as soft templates. Another common nanostructures and morphologies obtained are nanowires and nanosheets [66].

2.2.2. Pyrolysis/Carbonization of Organic Precursors

It consists of a cost-effective and mass production combustion process, in which QDs are nucleated and grown by exposing organic molecules to high temperatures [68]. Organic compounds, such as coffee grounds, glycerol or citric acid are frequently used as precursors in pyrolysis processes to obtain 2DQDs, such as GQDs and glutathione-functionalized GQDs (GQDs@GSH), making this process environmentally friendly [29,34,69].

2.2.3. Chemical Vapor Deposition (CVD)

A direct synthesis to produce GQDs with controlled growth parameters (temperature, pressure, time) and proper substrate (such as, copper or nickel) inside furnaces. Although relatively expensive, due to the requirement of high temperature, vacuum and restrict usage of specific substrates, the process is simple and the source can be either liquid or gaseous precursors. Among the advantages of this technique, one can highlight high quality, purity, and more controlled properties of products [33,63].

2.2.4. Colloidal Chemical Synthesis

Colloidal semiconductor QDs have been synthesized by wet chemistry methods using molecular precursors and can possess up to 10^8 atoms with diameter of the order of ~100 nm. The surface treatment of QDs with specific ligands allows physic-chemical stability and change the electronic properties of the material [70]. In a facile colloidal chemical route, ammonium tetrathiomolybdate ($(NH_4)_2MoS_4$) is used as precursor combined with oleyl amine (OLA), which acts as both reducing as well as stabilizing agent. The resultant hydrophobic material (MoS_2 monolayers) is further functionalized with cationic surfactants and transferred to an aqueous phase in order to obtain MoS_2QDs with good dispersability, low toxicity, and great photoluminesncence properties, being promising for applications in bioimaging. Cd-based quantum dots and rare-earth doped nanocrystals are also obtained using colloidal chemical routes [71,72].

2.2.5. Other Approaches

Amidst other techniques, chemical synthesis and ruthenium-catalyzed cage opening of fullerene are alternative bottom-up techniques used to synthesize 2DQDs. These techniques are more complex and require prevention against aggregation of materials in the final steps [29].

3. Functionalization of 2D Quantum Dots

Numerous strategies have been demonstrated to provide surface modification of 2DQDs, allowing to modify their properties and further improve their performance in distinct applications. Examples include enhanced solubility and reactivity, and enriched optical and electronic properties, making functionalized 2DQDs more attractive for advanced technology applications, such as cancer therapy, bioimaging, biosensing, optoelectronics, and energy storage systems [73]. Overall, 2DQDs can be functionalized via surface chemistry or interactions in order to module their properties. The introduction of oxygenated functional groups on 2DQDs induce the formation of QDs with much smaller dimensions due to the stronger reactivity of oxygen-based species [74]. The most popular functional groups attached to 2DQDs are S-H, COOH, COO^-, and C=S [75], and the edges of 2DQDs particularly act as excellent anchors for coupling molecules due to their highly defective nature [45]. For example, some studies have suggested that N and/or S doped GQDs have high electrocatalytic activity and conductivity for lithium batteries (see Figure 4a) [76–78]. Also, GQDs functionalized with carboxylic groups have great affinity for water, and therefore, have been demonstrated as biocompatible materials with boosted ability for covalent bonding with biomolecules for diagnostic purposes [45].

The functionalization of the edges of GQDs with antibodies or peptides has been demonstrated as crucial in cytotoxicity studies for imaging specific cancer cells and toxicology studies. For example, insulin conjugated GQDs have been used as specific labelling and dynamic identification of insulin receptors in 3T3-LQ adipocytes [79] (see Figure 4b). Experiments on surface chemistry functionalization or reduction of GQDs with low toxicity to MC3T3 cells enable to modulate the surface chemical groups and tune their photoluminescence response. Specifically, blue luminescence is observed for GQDs with edges functionalized with alkylamines. Upon reaction, the original –COOH and epoxy groups of GQDs are replaced by –CONHR and –CNHR groups. Blue luminescent reduced GQDs are obtained when sodium borohydride ($NaBH_4$) is used as reducing agent, transforming

carbonyl, epoxy, and amide moieties into –OH groups and minor surface defects (see Figure 3c) [15].

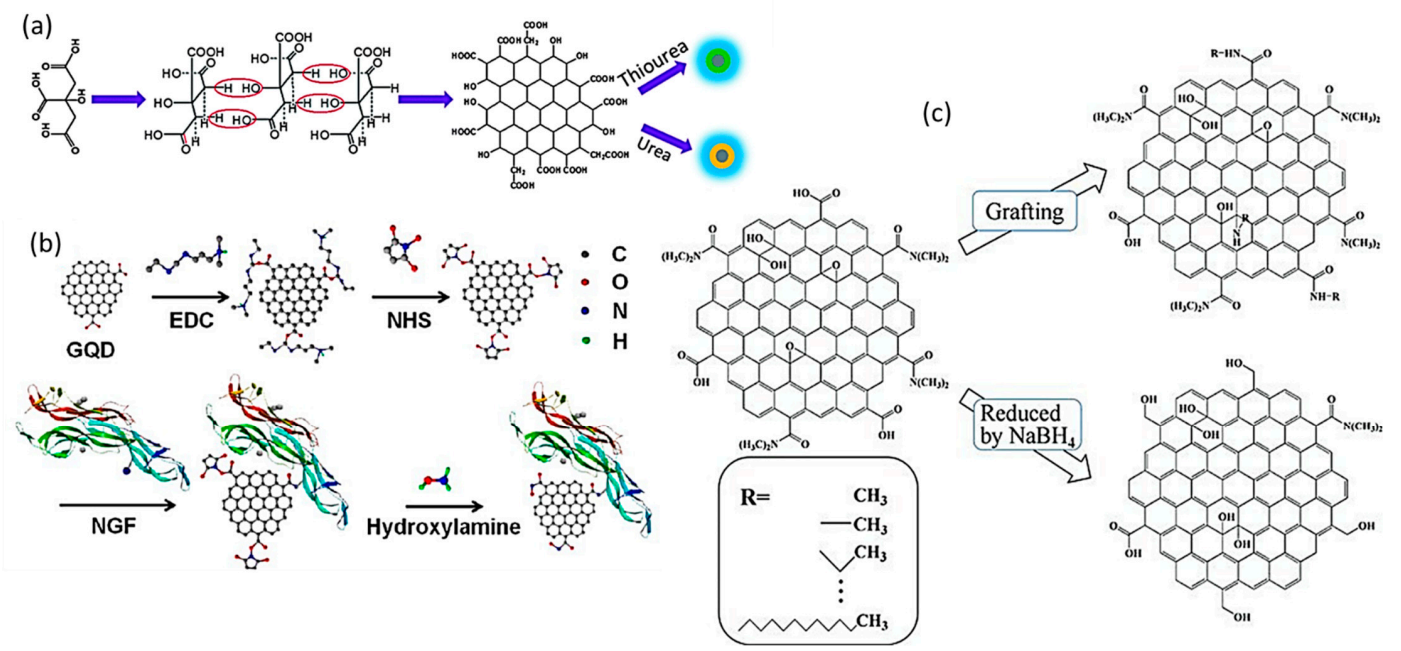

Figure 4. Scheme of functionalization synthesis of 2DQDs. (**a**) Growth mechanism of N doped GQDs (N:GQDs) and S,N co-doped GQDs (S,N:GQDS) by using citric acid (CA) as carbon source and urea and thiourea as N ang S sources. Reprinted with permission from [76]. (**b**) Route for conjugation of GQDs with a protein or peptide using nerve growth factor (NGF) as example. Reprinted with permission from [79]. (**c**) Surface modification of GQDs (grafting): alkylamines groups connected QDs structure, resulting blue luminescence m-GQDs, and reduction using $NaBH_4$ to obtain blue luminescent r-GQDs. Reprinted with permission from [15].

Because of their relatively small size (large specific surface area), 2DQDs can interact with cells through different mechanisms, such as endocytosis, pinocytosis, and phagocytosis [80]. Therefore, experimental and theoretical studies have been performed in order to verify whether such nanomaterials are suitable for nucleic acid delivery applications [81]. From experiments, GO has shown to be less cytotoxic than pristine graphene [82,83], however, the levels of oxidation and surface chemistry functionalization of GO sheets are decisive on different cytotoxicity and genotoxicity levels [84–86]. In another work, GQDs were functionalized using boric acid ($H_3BO_{3(s)}$), using a bottom-up molecular fusion method based on nitratred pyrenes. The resultant material (B-GQDs) has superior optical properties and long-wavelength PL emission with high quantum yield (Φ), being promising for luminescent composites in luminescent solar concentrator applications [87].

From theoretical studies, molecular dynamics (MD) simulation and density functional theory (DFT) calculations have been used to test how DNA molecules interact with GQDs and functional groups [41]. Other theoretical simulations have been performed in order to understand the effect of functional groups, such as OH-, SH, and NH_2, in 2DQDs. The use of density-functional theory (DFT) revealed that the functionalization on B and N atoms of BNQDs changed their bandgap and the semiconducting states, indicating that the electronic states are modified by the presence of functional groups [88]. DFT calculations also suggested that the light absorption of 2DQDs based on BP is tailored by the introduction of other functional groups, such as benzene rings and anthracene [89]. Hydrogen (H_2) evolution applications have also attracted attention of researchers that developed a novel hybrid photocatalyst comprising of cadmium selenide (CdSe) quantum dots (CdSe-QDs). Briefly, CdSe-QDs are supported with strong affinity on thiol (-SH) functionalized graphitic carbon nitride (g-C3N4) sheets (TF-g-C3N4). The functionalized heterostructure (CdSe-TF-g-C3N4)

demonstrated enhanced photocatalytic rate of H_2 generation, optimum morphology due to intimate interfacial attachments [90].

4. Photoluminescence Properties of 2D Quantum Dots

The fluorescence phenomenon has been intensively explored since it was first observed by George Gabriel Stokes in 1852 [91]. In a simple experimental setup, Stokes demonstrated that fluorite glows in the dark upon illumination by ultraviolet (UV) light. He named this process as fluorescence [92]. A simple way to describe the photoluminescence (PL) phenomenon is shown in Figure 2. A 2DQD of size L can be seen, in first approximation, as a potential well with infinitely high walls infinite. Quantum mechanics tells us, that, in such confined geometry, the electronic states will be quantized (Equation (1)). The PL mechanism (see Figure 2b) involves a photon with energy Ei (and frequency υi) being absorbed (1) by an electron in the QD; (2) the excited electron can decay by emission of phonons (thermal vibrations) via non-radiative mechanisms, without producing light; (3) the electron recombines with the hole emitting a photon with lower energy Ef (and frequency υf).

The aromatic and conjugated molecular groups capable to absorb UV light and present fluorescence are called fluorophores. Interest around the mechanism of fluorescence (nomenclature used by chemists to indicate the absorption and emission of light by atoms or molecules) and PL (nomenclature used by physicists to depict the absorption and emission of light by semiconductor) is due to the interest in application of photoluminescent materials in areas that range from chemistry to biology [93]. For QDs, the luminescence appears from the recombination of electron-hole (e-h) pairs through radiative routes, known as exciton decay. However, for non-radiative routes, such decay may diminish the fluorescence yield. Henceforth, in order to enhance the efficiency of PL in QDs and modify their photo-physical properties, core shell-typed QDs techniques may be used, in which shells of different semiconductors with larger band gaps are grown as coatings [20].

Equally important, 2DQDs also present PL effect [15,22,94]. This can be seen in Figure 5a, comparing PL mechanism occurred in carbon-based quantum dots and semiconductor quantum dots (SQD) [37]. Likewise, Figure 5b illustrates the size-dependent PL spectra with excitation source of 325 nm for GQDs in deionized (DI) water. It is clear that the peak energy and the shape of the spectra depend on the size of GQDs. The inset image shows different luminescence effect observed for different sizes of GQDs. Figure 5c indicates the excitation-wavelength-dependence of shifts in PL peaks for different sizes of GQD, in which similar behavior of peak shifts is present, regardless the excitation wavelength, except for 470 nm [36].

The quantum yield (Φ) is defined as the ratio of number of photons emitted to the number of photons absorbed by a material. The quantum yield quantifies how efficient is the photon emission for fluorescent or photoluminescent materials. In Table 1, the main categories of 2DQDs are summarized, including synthesis methods and quantum yield. It has been reported that heteroatom doping, surface passivation, and edge effects have great influence to considerably increase the Φ in 2DQDs. Generally, the higher is the Φ, the most promising is the use of 2DQDs for biological and optoelectronic applications [22].

It has been demonstrated in vitro and in vivo that QD-tagged reduced graphene oxide (QD-rGO) nanocomposite can be used in cell/tumour bioimaging with photo-thermal therapy due to its strong fluorescence and low toxicity [47]. The fluorescence bioimaging and photothermal therapy provide in situ monitoring, and nanocomposite can act as a cell killer, being promising for cancer treatment and diagnosis. Such nanocomposite generates heat, which is an extremely useful characteristic for photo-thermal therapies, especially as it also allows in situ heat/temperature sensing. It was demonstrated that, for samples prepared at equal molar concentrations (3.4×10^{-4} mmol), the PL response of rGO-QDs is dependent on the size of the 2D material. Figure 6a,b show that regardless the wavelength of the excitation/emission energy source, the fluorescence of ultra-small rGO (US-rGO—38 nm) and small rGO (S-rGO—260 nm) are 15% and 50% lower, respectively,

than the fluorescence of pure QDs. The size dependent fluorescence effect of rGO-based QDs is illustrated in Figure 6c. A 350 nm laser wavelength coming from below the planar sheets results in different fluorescence effect according to size dimensions of the material (less fluorescence from larger—260 nm—than smaller sheets—38 nm) [47].

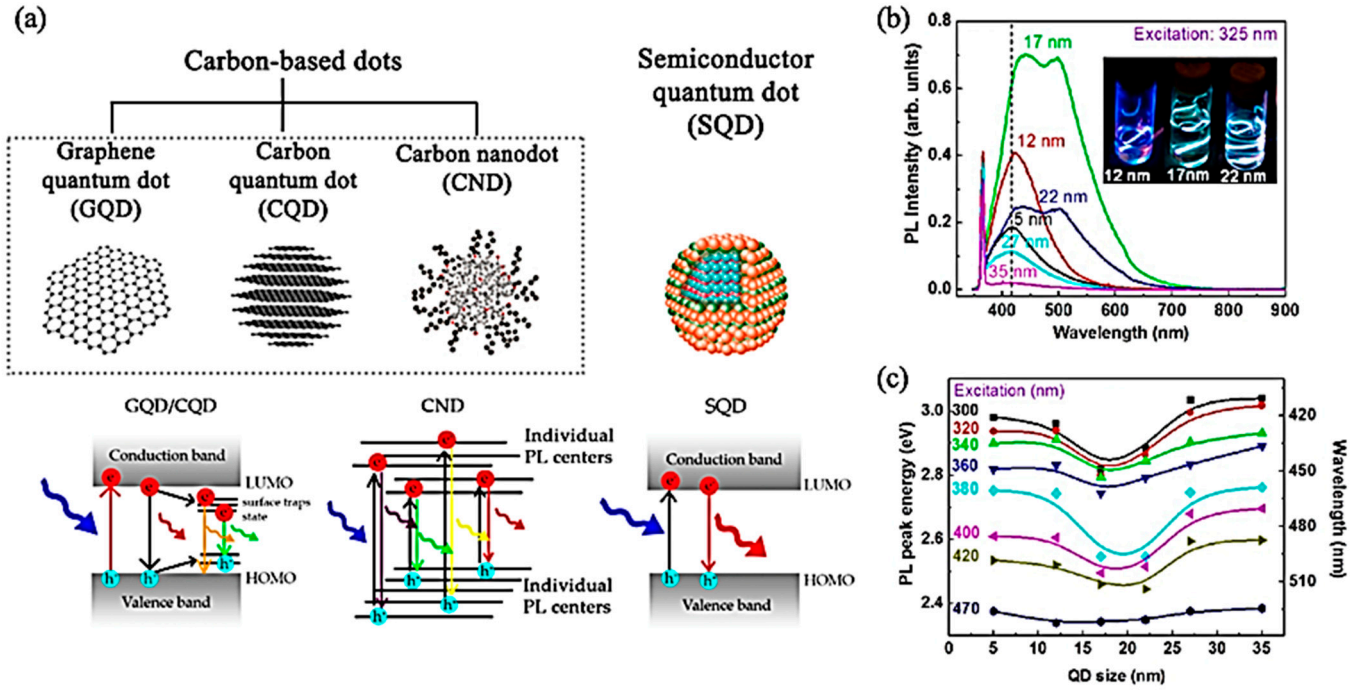

Figure 5. (**a**) Schematic illustration and PL mechanism of carbon-based dots: GQDs, carbon quantum dots (CQDs), carbon nanodots (CNDs)) and semiconductor quantum dots (SQDs). Reprinted with permission © 2017 by MDPI [37]. (**b**) Size-dependent PL spectra with excitation source of 325 nm for GQD in DI water. The inset shows the different luminescence effect with colors varying according to average size of QD (12 nm, 17 nm and 22 nm). (**c**) Dependence of PL peak shifts ranging with excitation wavelengths ranging from 300 to 470 nm for GQD with different sizes. Adapted and reprinted with permission. Copyright © 2012, American Chemical Society [36].

Table 1. Categories, synthesis, and quantum yield (Φ) of 2DQDs. Adapted with permission © 2018 Elsevier Ltd. All rights reserved [22].

Categories	2DQDs	Approach	Synthesis	Φ (%)
Single-element 2DQD	Carbon dots (CDs)	Bottom-up	Hydrothermal method	80
		Bottom-up	Solvothermal method	11.4
		Bottom-up	Microwave radiation	11.7–22.9
	Graphene quantum dots (GQDs)	Top-down	Chemical etching from coal precursor	0.6
	Phosphorene quantum dots (PQDs)	Top-down or bottom-up	Sonication and solvothermal	8.4
		Top-down	Sonication	N/A
Double-element 2DQD	TMDs (MoS_2, WS_2) quantum dots	Top-down	Chemical etching by acid	>95
		Top-down	Ultrasonication	N/A
		Top-down	Lithium intercalation	N/A
Multi-element 2DQD	MXene-type quantum dots	Top-down or bottom-up	Hydrothermal method	10

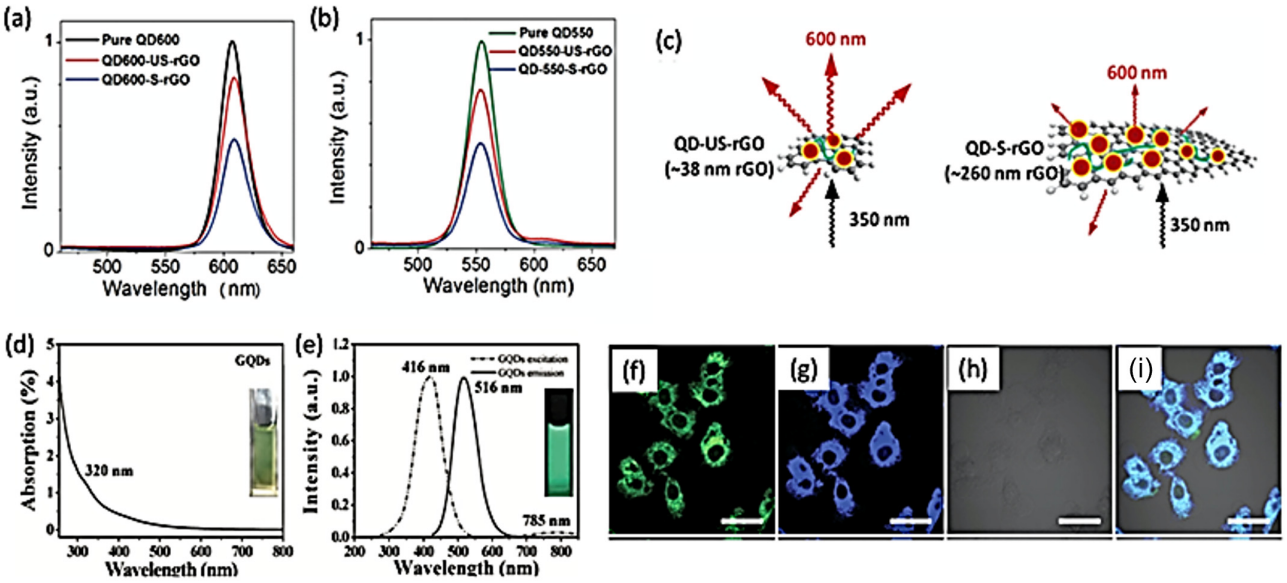

Figure 6. Fluorescence spectra of pure, small (S-rGO) and ultra-small (US-rGO) reduced graphene oxide quantum dots emitting at (**a**) 600 nm, and (**b**) at 550 nm. (**c**) Schematic for the surface adsorption of graphene oxide using an amphiphilic polypeptide (poly(L-lysine)) with the correspondent adsorption and conjugation. Reprinted with permission [47]. (**d**) UV-Vis absorption (UV-Vis ABS) spectra of graphene quantum dots (GQDs)—inset image: photograph taken under visible light. (**e**) Optimal excitation and emission PL spectra of GQDs—inset image: photograph taken under 365 nm UV light Reprinted with permission and adapted. [15]. (**f**) Confocal laser scanning microscopy image (CLSM) of HeLa living cells stained with 0.001 mg/mL of lysotracker for 20 min for MoS_2/WS_2 quantum dots. (**g**) CLSM image of HeLa living cells incubated in DMEM (Dulbecco's modified eagle medium) containing 50 μ/mL. (**h**) The corresponding bright field image and (**i**) overlapped image of the living cells. All scales are 40 μm. Reprinted with permission and adapted [16].

The reduction of dimensions of graphene, leading to GQDs, can tune its bandgap from 0 eV in macroscopic samples to values comparable to the energy gaps in benzene molecules (around 3.1 eV). Consequently, the luminescence effect of GQD is manifested with many advantages relative to traditional fluorescent materials. For instance, great attention has been addressed to GQDs due to their optical activity, chemical stability, reasonable biocompatibility and low cytotoxicity. Previous reports correlate the luminescence phenomenon to quantum size effect, zig-zag edges, and defects in the structure of graphene. For example, GQDs have been synthesized by solvothermal reactions with radical groups bonded to their edges, leading to surface modifications causing various optical properties [15]. The green luminescent spectra of the surface modified GQDs for absorption and emission induced by defect state emission can be seen in Figure 6d,e. The ultraviolet visible spectroscopy (UV-Vis) analysis shows a shoulder peak at 320 nm Figure 6d attributed to surface passivation and the fluorescence spectra indicate that GQD have optimal excitation and emission wavelengths at 416 nm and 516 nm, showing the green fluorescence under UV light.

More recently, it was shown that uniform MoS_2/WS_2 QDs with average size of 3 nm can be prepared by the combination of sonication and solvothermal treatment of bulk materials at room temperature. Such hybrid QDs are dispersed in water with great stability and present strong fluorescence, low cytotoxicity and good biocompatibility, higher surface area and several edged atoms. Figure 6f–i show MoS_2/WS_2 quantum dots as fluorescent probes interacting with living cells for bioimaging, indicating their potential application as cell-imaging agents and probes for in vitro imaging in biomedicine [16]. Some other studies have been performed to better understand the PL properties and the electrochemiluminescence (ECL) features of boron nitride quantum dots (BN-QDs) [40,74]. In particular, tunable blue/green PL with different size dimensions can be created by sonication-solvothermal

treatment of bulk BN in different organic solvents. The as-prepared BN-QDs serve as fluorescent sensing agent for label-free detection of ferric ions (Fe^{3+}), HeLa cells bioimaging, and fiber staining, whereas ECL properties were detected in BN-QDs using cysteine as coreactant [74].

There are many other studies investigating the fluorescence properties of other 2DQDs. For example, CdSe quantum dots have shown size-tunable emission of light in the visible region spectrum. In a brief, the PL effect of CdSe-QDs originates from different factors: (1) exciton recombination at the band structure, that is transitions from the lowest unoccupied state of orbitals of Cd, to the highest occupied state of orbitals of Se, (2) deactivation of electrons previously excited, and (3) surface states. By investigating the band structures in CdSe-QDs, PL behaviour can be observed. In general, spectral shits of CdSe-QDs are commonly attributed to size variations, temperature, pressure, and dielectric environments. Such factors influence on the quantum confinement of excitons and changes on the bandgap energies, especially due to exciton-phonon coupling, confinement energy, surgace charges, and surface chemical changes [95].

In fact, photo luminescent GQDs with wavelength-controllable emissions and fluorescence colour tuneable by excitation wavelength modifications are generally easy to obtain and can be made environmentally-friendly. Moreover, they usually present a strong fluorescence effect, and many other useful properties, such as low-toxicity, high biocompatibility, reasonable chemical inertness and high aqueous solubility, as well as superior resistance to photo bleaching, making them promising for biomedical applications, illumination and display techniques [94].

Remarkably, surface chemistry approaches make possible to enhance the PL effect of 2DQDs. The presence of different radical groups attached to the surface of GQDs, for instance, can diminish or enlarge non-radiative recombination, and transfer electrons from the defect state emission to the intrinsic state emission. As such, PL mechanism and fluorescence can be notably changed through surface chemistry alterations [15,16,47]. Still, much more can be done for understanding the PL in 2DQDs. The PL effect is still a debatable topic due to the complexity of quantum confinement effects, the influence of defects, and edges states of 2D materials. Additionally, the impact of environmental conditions such as temperature, pressure, pH, among others have been demonstrated to play a fundamental role in the properties of 2DQDs, which directly affect the possibilities for applications [48]. In this context, the selection of appropriate characterization techniques is essential to differentiate qualitatively and quantitatively the various synthesized materials, understand and analyse their different structure and properties, to effectively apply them into specific fields.

5. Fundamental Characterization Techniques of 2D Quantum Dots

Generally, analytical methods are used for characterization of QDs, including microscopy, diffraction and spectroscopy techniques. In Table 2, a list of the most commonly used characterization techniques for 2DQDs and their usage propose is shown below.

Table 2. C Common characterization techniques and their usage propose for 2DQDs. Copyright © 2015 WILEY-VCH Verlag GmbH & Co. KGaA, Weinheim [16].

Technique	Acronym	Applied for Analyzing:
Transmission electron microscopy	TEM	Particle size distribution, crystalline organization
High-resolution transmission electron microscopy	HRTEM	Crystallinity, d-spacing, planes
Energy dispersive X-ray spectroscopy	EDX	Detection of elements

Table 2. *Cont.*

Technique	Acronym	Applied for Analyzing:
X-ray photoelectron spectroscopy	XPS	Understanding chemical states and compositions
Atomic force microscopy	AFM	Morphology and thickness
X-ray diffraction	XRD	Crystal structure, unit cell dimensions, crystal spacing.
Raman spectroscopy	-	Measuring the rotational, vibrational, and other low-frequency modes, and other defect states.
UV-Vis spectroscopy (or spectrophotometry)	UV-Vis	Optical properties (light absorption and transmission), qualitative information (size and concentration).
Photoluminescence spectroscopy	PL spectroscopy	Electronic transitions, estimation of quantum yield.

Atomic force microscopy (AFM) is commonly used to image the surface of any type of material (from polymers to ceramics), as well as to investigate their mechanical properties and their adhesion strength. It guarantees a meticulous and detailed analysis of morphology and structural properties, since the morphology and topography of materials can be analyzed in three-dimensions using a probe tip (in the range of 1 nm to 200 nm) that images the surfaces [96]. This technique also allows the measurement of the number of layers of nanomaterials (graphene—0.34 nm theoretical thickness for a monolayer), by analyzing the height distribution profile as shown in Figure 7a. Specifically, the red line in Figure 7a provides the height profile curve of GQDs, and the statistical analysis based on more than hundreds of samples, showing that more than 90% of GQD are monolayer with thickness ranging between 0.5 and 1.0 nm [37].

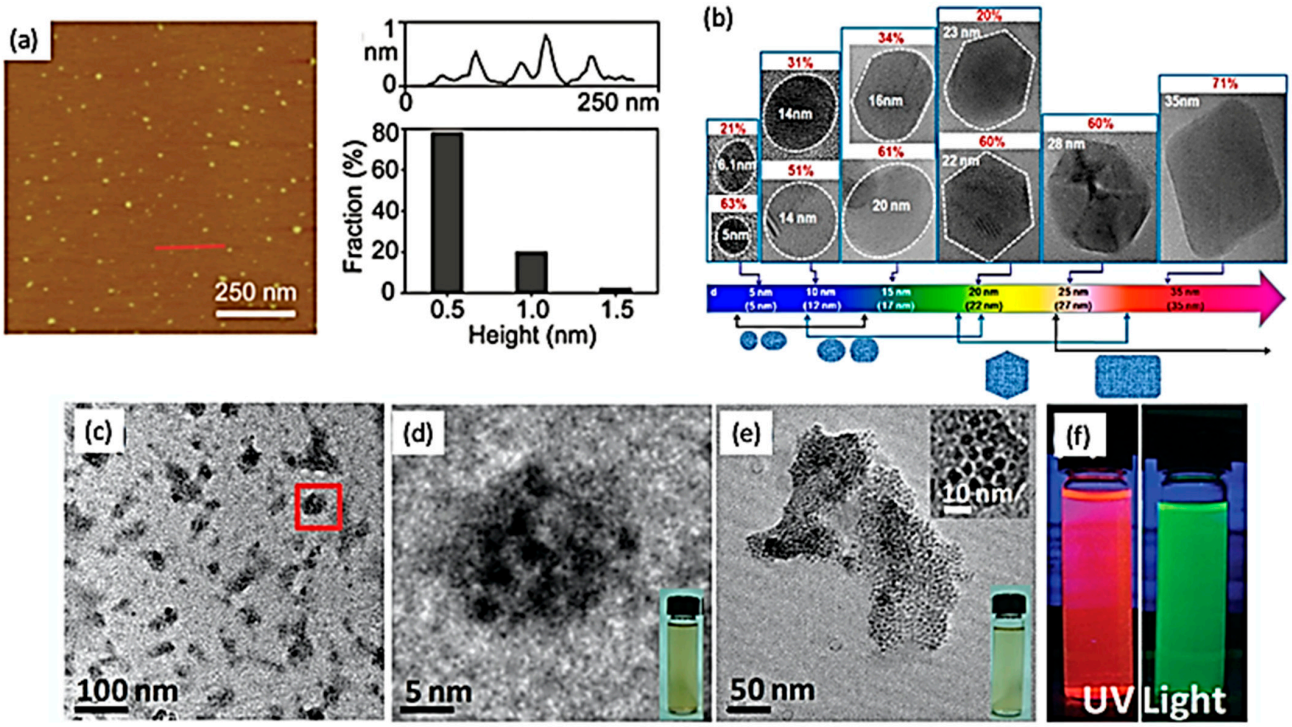

Figure 7. Images of 2DQDs obtained by AFM, TEM and HR-TEM characterization techniques. (**a**) AFM image, height profile and height distribution of GQDs. *Reprinted with permission from* [37].

(**b**) HR-TEM images of GQD for different shapes and corresponding populations with increasing their average size. The dashed lines indicate the size dimension of GQDs. *Reprinted with permission from* [36] *Copyright © 2012, American Chemical Society.* (**c**) TEM image of reduced graphene oxide quantum dots (rGOQDs). (**d**) HR-TEM image of the area shown in Figure 7c. (**e**) TEM image of rGOQDs with a higher resolution image of an area un the upper right inset. The insets at the lower right of Figure 7d,e show the sample suspension under visible light. (**f**) Suspension of rGOQDs under UV light exposure. *Reprinted with permission from* [47].

High-resolution TEM (HR-TEM) is used to analyze 2DQDs and allows to classify their predominant shapes, since it provides images with atomic resolution (atomic arrangement and interplanar/lattice spacing). It has been demonstrated that circular and elliptical GQDs in the range of size between 5 nm to 12 nm can be produced with a yield of more than 50%, as it can be seen in Figure 7b [36]. It was shown that circular GQDs are uncommon whereas elliptical shapes are more frequent for sizes of 15 nm, with 1/3 of them having irregular shape. Particularly, most GQDs with sizes between 20 nm to 35 nm have hexagonal or rectangular shape with irregular rounded sides and vertices. These atomic features are visualized by HRTEM with clear distinction, providing detailed information about edge shapes (such as zig-zag and armchair edges), and correlating with their actual shapes.

It was demonstrated that QDs-rGO nanocomposites synthesized by surface chemistry routes can present distinct sizes, according to specific reactions conditions [47]. Figure 7c–e show HR-TEM images of the QDs-rGO s in different scales, where the red square in Figure 7c shown in 100 nm scaled image represents the zoom-in in 5 nm image. It was demonstrated that QDs do not aggregate after synthesis (see Figure 7e), which is an important characteristic for practical applications. Apart from that, QDs-rGO present a quasi-regular 2D array structure with no visible cracks, indicating reasonable interface adhesion. The fluorescence of QDs-rGO is shown in Figure 7f, in which two liquid suspensions made of two-sized materials were illuminated with UV light. Besides the color, the density of QDs were switched with a concentration variation in the solution.

The results acquired from XRD are complementary to microscopic and spectroscopy techniques, such as for phase identification, purity degree, crystallite size, and morphology. To give an example, the identification of crystalline planes and d-spacing can be obtained by analyzing the diffraction peak of GQDs. It has been shown that QDs-rGO have large d-spacing values, indicating the presence of oxygen functional groups. By further interpreting the diffraction peak, as for calculating its full width at half maximum (FWHM), one can extract the average diameter of the crystallite size of synthesized GQDs to be around 2 nm [97]. XPS has been widely used to investigate the oxidation state of elements present in 2D materials. The high resolution XPS spectra corresponding to C1s (285 eV) and O1s (533 eV) have been identified for GQDs with different shape as comparing to graphite. After deconvolution of C1s peak, four main features are noted: sp2 carbon (CQC, C-C) at 284.6 eV, sp3 carbon (C-OH) at 285.9 eV, C-O-C at 287.3 eV, and C=O at 289.61 eV, which is an indication that oxygen functional groups were attached to graphene sheets during the reaction, and defects were detected in GQDs, as revealed by the resolution of sp3 carbon peak. The XPS spectrum of O1s is mainly resolved in two peaks, at 532.7 eV (CQO) and 534.4 eV (C-O), further confirming that GQDs are rich in oxygen functional groups content [98–100].

The properties and functionalities of nanomaterials are significantly different comparing to their macroscopic bulk counterparts for two main aspects: (i) the higher surface area over volume ratio favors their chemical reactivity, and (ii) the presence of quantum phenomena dominate the interactions of matter at such smaller dimensions. Understanding the structure and properties of nanomaterials combining qualitative and quantitative characterization techniques is crucial for designing and engineering materials for a given application [101,102].

6. Applications of 2D Quantum Dots

The long-term consequences of nanomaterials on human body are of great concern on governmental agencies and scientists working in the biomedical field. Over the past few decades, the number of applications based on nanomaterials has increased dramatically, from consumer products, manufacturing processes, and medical products. Therefore, it is crucial that workers and end-users have appropriate protection of potential risks involving such materials, since the exposure to nanomaterials is substantial and increasing, studies involving the toxicological properties is fundamental [103]. The toxicity of QDs depends on parameters, such as size dimensions, preparation methods, dosage, administration route, residual contents, and environmental conditions [4].

As it has been previously said, the particular dimensions, chemical structure, and resulting electrical and optical properties of 2DQDs make these materials tremendously attractive for nanotechnologies. Over a wide range of possible applications, one can list photo electronic devices, energy storage and conversion systems, electrochemistry, capacitors, catalysis, and photodetectors [20,29,36,104]. Special attention has been devoted for the fabrication of highly selective and sensitive biosensors based on 2DQDs owing to their unique properties, including excellent biocompatibility, chemical stability, low toxicity, structural flexibility, electronic properties, and photoluminescence properties [46,105].

The potential biological toxicity of 2DQDs has been evaluated by in vitro and in vivo imaging due to their chemical composition and nano-size dimensions [106,107]. Obtaining in vivo systems analysis is a much complex and expensive task than assessing toxicity in in vitro cell cultures. In vitro cytotoxicity of GQDs has been evaluated with MC3T3 cells by methylthiazolyldiphenyltetrazolium bromide (MTT) assay, indicating that GQDs and r-GQDs have extremely low toxicity to MC3T3 cells with relative cell viability variation due to methylamine groups affecting the cells [15]. In another in vitro *cytotoxicology* study, MoS_2-QDs prepared by sodium (Na) intercalation reaction were used as fluorescent probes for long-term tracing of live cells [108].

Zebrafish (Dnaio rerio) has been popularly applied in toxicity studies of various nanomaterials as an in vivo system due to fastness, reliability, cost affordability, optical transparency, and high homology to the human genome [109,110]. In a recent study, the developmental toxicity of zebrafish embryos exposed to GQDs has shown that there is a concentration-dependence on the potential nanotoxicity of GQDs. After exposure to GQds (0, 12.5, 25, 50, 100, and 200 μg/mL) for 4 h-96 post fertilization (hpf), it has been demonstrated that the mortality of zebrafish embryos increased, while their hatchability, heart rate, and spontaneous movement decreased, with persistent effects due to concentrations higher than 50 μg/mL [111]. Other studies suggested that MoS_2 and WS_2 have low cytotoxicity levels in a series of biocompatibility tests, including live-dead cell assays, reactive oxygen species generation assays, and direct assessment of cellular morphology of TMD-exposed human epithelial kidney cells (HEK293F). Also, genotoxicity and genetic mutagenesis were tested with bacterial strain S. typhimurium TA100. Both materials are deleterious to cellular viability and do not induce genetic defects, appearing to be biocompatible for future application in medical devices [112].

Table 3 shows a summary of examples of 2DQDs in the application in biosensing and imaging. Overall, 2DQDs add a great value to the biosensing and bioimaging technologies, since they emit in the whole spectrum and show low degradation over time compared to traditional organic dyes [113]. Here, we focus on their applicability for biosensing, bioimaging purposes, as well as theranostic applications of 2DQDs.

Table 3. Applications of 2D quantum dots and examples of toxicity tests performed with the corresponding outcomes for each study.

2D Quantum Dots	Toxicity Test	Outcome	Applications	Ref.
GQDs	In vitro	Photoluminescent GQDs with low toxicity to MC3TW cells obtained by tuning surface chemistry routes.	Strong tool in biomedical field, for up-conversion imaging.	[15]
GQDs	In vivo	Fluorescence agents showing efficiency for treatment of cancer cells and tumours	Fluorescence contrast agents for bioimaging	[93,114]
GQDs	In vivo	Concentration dependence on the potential toxicity of GQDs to zebrafish embryos	Biological and medical, such as bioimaging, biosensing, and drug delivery.	[108–110]
GQDs/polyethylene glycol(PEG)/MoS2-	In vivo/in vitro	Fluorescent biosensor for epithelial cell adhesion molecule (EpCAM) detection	Drug delivery	[115]
MoS_2-QDs	In vitro	Strongly fluorescent, highly photo-stable QDs with low toxicity	Fluorescent probes for long-term live cell tracing	[107]
MoS_2-QDs	In vitro	Human cervical cancer cells (HeLa) model showed good biocompatibility with no obvious cytotoxicity when concentration ranges from 15 to 100 µg/mL	up-conversion bioimaging	[116]
MoS_2/WS_2 QDs	In vitro	Low cytotoxicity levels in biocompatibility tests, being deleterious to cellular viability and not inducing genetic defects	Medical devices	[111]
BN-QDs and BCNO-QDs	In vitro	Fluorescence detected under 405 nm excitation for labelling HeLa cells	Bioimaging probes	[117]
PEGylated-BPQDs	In vitro	Low toxicity when integrated into single component platform with fluorescence approach to image cancer cells	Bioimaging probes	[118]

6.1. Biosensing

A biosensor is any device that assures detection, transduction and generation of signals from materials through a bioactivity-based receptor. The first biosensors invented were simplistic devices for monitoring blood gas levels of surgical patients [105]. The recent advances in technology enabled the fabrication of highly sensitive, selective and cost-effective biosensors introduced into biomedical field to enhance quality of life of patients and users. Examples of their utilization include but are not limited to detection of diseases, drugs, glucose, home pregnancy tests, and food safety monitoring. Many efforts have been directed to design biosensors with reproducible analysis in real time, with higher sensitivity and selectivity [38,119,120].

Carbon nanomaterials, such as carbon nanotubes (CNT), graphene and its derivatives, carbon dots (CD) and GQDs, have been applied in fluorescence biosensing. Since these materials present reasonable sensitivity of biological and chemical properties, efficient biosensors with superior performance can be developed. In particular, GQDs have high electron mobility, chemical stability, apart from excellent properties of luminescence, which

can be activated by proper interaction with chemical groups, cations or anions [93]. Some examples of GQDs as platforms for biosensing activities are the development of DNA detection sensors [121], and the synthesis of highly blue-luminescent nitrogen doped GQD used as fluorescent probe to detect glutathione (GSH), an abundant thiol with antioxidative properties that protects animal cells against damages [122]. A fluorescent probe based on a silver nanoparticle graphene QD nanocomposite (AgNP-DNA@GQD) was used to detect glucose and H_2O_2 (see Figure 8a) [115]. In particular, the usage of such biosensor could be extended to detect glucose in human urine with an ultra-sensitive quantitative analysis. Since GQDs biosensors have the ability to bind to several biomolecules, they have been fabricated on the limit of detection, sensitivity, selectivity, repeatability, and biocompatibility [38]. A fluorescent biosensor based on GQDs/polyethylene glycol (PEG)/MoS_2 for epithelial cell adhesion molecule (EpCAM) detection was developed [123]. Such designed sensor can be used for drug delivery applications, as it can be seen in Figure 8b [32,38].

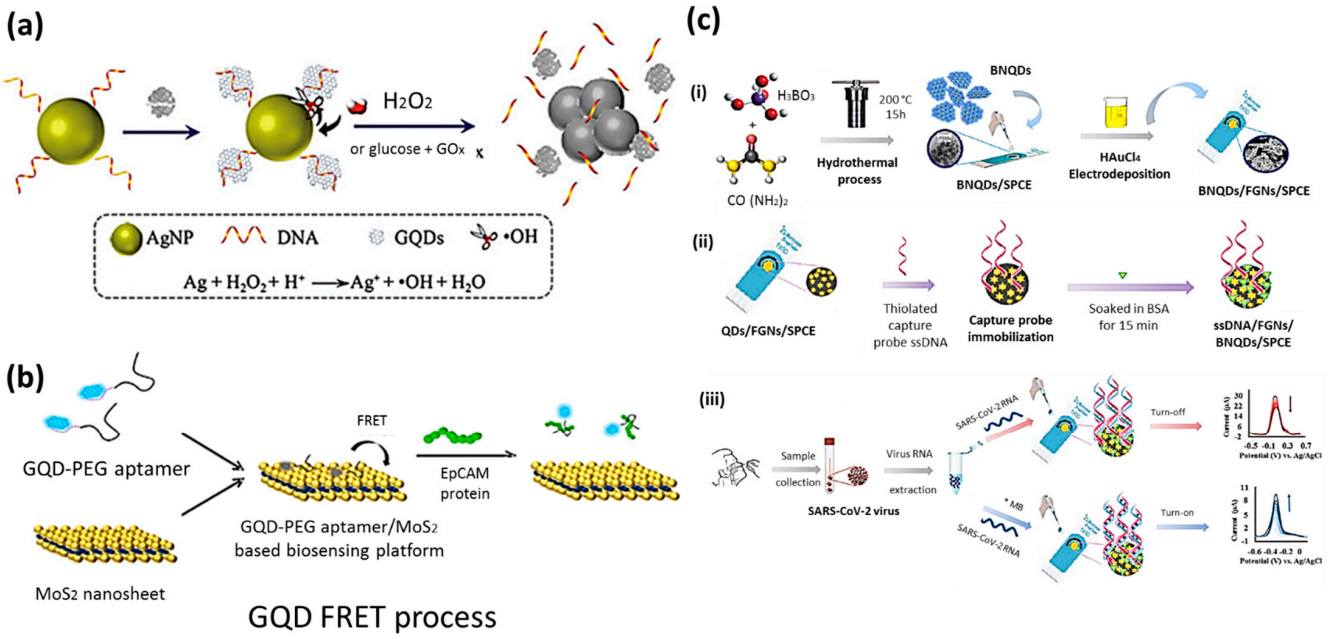

Figure 8. (**a**) Schematic representation of a fluorescent biosensor based on silver nanoparticles graphene QDs nanocomposite for detection of glucose and H_2O_2. Reprinted with permission from [37]. (**b**) Fluorescence resonance energy transfer (FRET) biosensor based on GQDs-PEG/MoS_2. Reprinted with permission from [115] *Copyright © 2016 Elsevier B.V. All rights reserved*. (**c**) Schematic representation of SARS-CoV-2 detection using an electrochemical biosensor based on BN-QDs/FGNs/SPCE. (**i**) synthesis of nanostructure based on BN-QDs, (**ii**) capture probe immobilization and electrode fabrication, and (**iii**) procedure for electrochemical detection Copyright © 2022 Elsevier B.V. All rights reserved [49].

The early detection and diagnosis of cancer are essential to provide appropriate treatment and guarantee higher chances of curability. Using a biomarker indicator, such as MUC1 (a transmembrane glycoprotein), can be extremely useful to detect breast cancer in early stages. Biosensors based on MoS_2-QDs are of great interest owing to the ability of transition metal ions generated by MoS_2 undergo fluorescence quenching when in contact with organic dye molecules. In a particular study, a FAM fluoreophore-labeled ssDNA fluorescent probe (P0-FAM) stacked on the surface of MoS_2 quantum dots with high sensitivity to MUC1 was constructed to locate breast cancer cells [124]. Recently, a biosensor based on BN-QDs, flower-like gold nanostructures, and screen-printed carbon electrode (BN-QDs/FGNs/SPCE) functionalized with antisense DNA olionucleotide has been shown as an alternative solution for clinical diagnosis of SARS-CoV-2 [49]. Overall, these biosensors are highly efficient for the identification of ions, and organic/inorganic molecules. Apart

from that, in vitro and in vivo bioimaging has been connected to biosensing toward the identification of specific biological components for diagnostic purpose [116].

6.2. Bioimaging

Bioimaging is a diagnostic tool used to assist and monitor biological activity of components. Biomedical studies are generally based on a visual detection of components, being carried out in two conditions: in vitro or in vivo environments. Techniques such as optical spectroscopy, fluorescence spectroscopy, photoacoustic imaging (PAI), positron emitting tomography (PET), and non-linear spectroscopy are commonly used for designing the imaging probes [116]. In contrast, several functional nanoparticles, such as semiconductor quantum dots, gold nanoparticles, magnetic nanoparticles, carbon nanotubes, and graphene nanosheets, have been used in diagnostics, imaging, and therapy [16].

Despite dyes and semiconductor QDs have been widely used for bioimaging of living cells, these materials present a photo-bleaching effect and high toxicity from heavy metals. Consequently, alternative and non-toxic materials are of extreme interest for bioimaging purposes. It is known that carbon nanomaterials present high aqueous solubility, biocompatibility, low toxicity and resistance to photo bleaching, so that they are promising candidates to replace traditional QDs [93]. Specifically, the PL effect, low toxicity and good biocompatibility of 2DQDs make them promising candidates for both in vitro (tumour cells imaging, targeted cellular imaging, etc.) and in vivo (GQD acting as fluorescence contrast in mice) bioimaging applications [94]. These analyses are further discussed below.

6.2.1. In Vitro Imaging

In vitro analysis are performed in tubes or glass vessels in a controlled environment rather than in living organisms. Since GQDs can infiltrate cells effortlessly, in vitro analysis of species using GQD-based biomarkers have been extensively deployed for imaging tumor cells. In a recent study, it has been demonstrated that GQDs can be used for imaging Hela cells (Figure 9a,b). Also, in vitro tests of MoS_2-QDs prepared by intercalating bulk MoS_2 using tetrabutylammonium (TBA) using human cervical cancer cells (HeLa) model have shown good biocompatibility with no obvious cytotoxicity when the concentration of MoS_2-QDs ranges from 15 to 100 µg/mL, demonstrating great promising for up-conversion bioimaging [117]. Beyond graphene and MoS_2-QDs, BN and boron carbon oxynitride (BCNO) quantum dots (BN-QDs and BCNO-QDs) have also been shown as promising bio imaging probes through labelling HeLa cell with fluorescence detected under 405 nm excitation [118]. In another study, water soluble PEGylated black phosphorous (BP) QDs have shown little toxicity when integrated into a single component platform and imaged cancer cells using an in vitro fluorescence approach [114]. Similarly, green luminescent GQD have been incubated with human breast cancer cell lines T747D with their nucleus stained with DAPI (4-6-diamidino-2-phenylindole di-hydrochloride) (see Figure 9c,d) [94].

6.2.2. In Vivo Imaging

In vivo analysis are biological experiments done with living organism environment, such as animals or human cells. It has been shown that it is possible to use 2DQDs as fluorescence contrast agents in mice for in vivo imaging. GQDs can be prepared by pyrolysis of L-glutamic acid for imaging. After subcutaneous injection into the back and intramuscularly into the leg of mice, bioimaging analysis showed that the fluorescence response can be measured. The resultant fluorescence images under several excitation and emission filters can be viewed in Figure 9e. In particular, this study showed that longer wavelengths are efficient for in vivo imaging analysis [94,125], suggesting that GQDs are efficient to help in the treatment of cancer cells and tumors. In a different approach, plant-leaf derived GQDs from neem (*Azadirachta indica*) were used to expose zebrafish embryos to evaluate the biosafety of GQ using an in vivo labelling approach for cell imaging studies. Such GQDs were demonstrated to be highly compatible to human cell imaging of cancer cells (MCF-7), normal human mammary epithelial cells (MCF-10A), and HeLa cells [44].

Renal carcinoma tumor cells (SW480) in kumming mice and BALB/c mice (4–5 weeks old) have also been successfully identified using fluorescence imaging and further investigated by a systematic study of the biocompatibility, biodistribution and metabolism route of MoS_2-QDs [43].

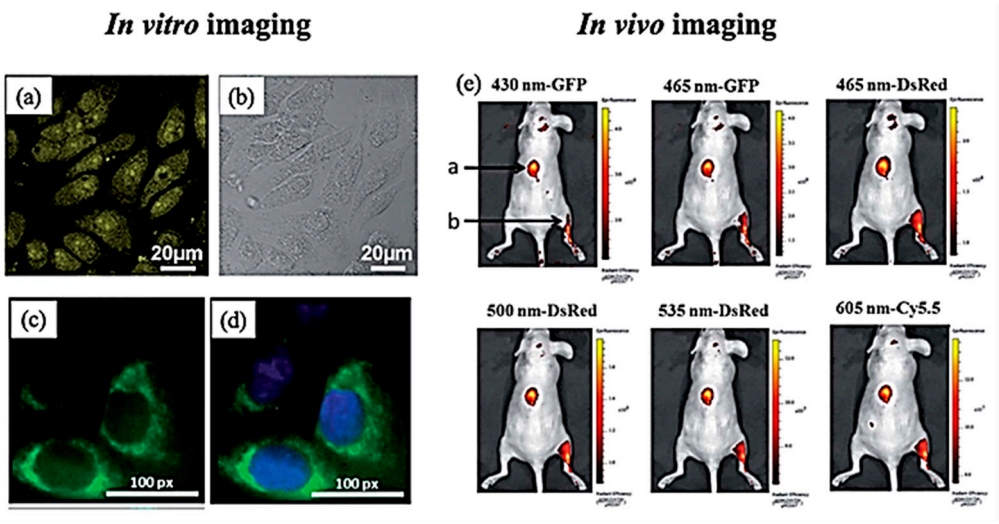

Figure 9. In vitro imaging (**a**) Confocal fluorescence microscopy images of Hela cells with boron-doped GQDs (B-GQD) coated with liposomes at the excitation wavelength of 405 nm, and (**b**) the corresponding image under bright field. Reprinted with permission from [125]. (**c**) Fluorescent images of agglomerated green GQDs surrounding nucleus of human breast cancer cell (T47D) after incubation for 4 h. (**d**) Overlapped blue DAPI and GQDs (green) stained high contrast image of nucleolus. Reprinted with permission and adapted. Reprinted with permission from [126]. In vivo fluorescence (**e**) images of mice after subcutaneous injection of GQDs (spot a) and intramuscularly injection (spot b) taken at various excitation and emission wavelengths. *Reprinted with permission from* [94].

6.3. Theranostic Applications of 2DQDs

By definition, theranostic approaches involve the combination of both diagnostic as well as therapeutic procedures, that is when a disease is first diagnosed, and later properly mediated and treated. Using 2DQDs for theranostic purposes is extremely advantageous since they allow easy identification of diseases, by monitoring health conditions and targeting cells. When applied as imaging probes and delivery vehicles, 2DQDs enable the detection of selected cells or tumours, with subsequent release of drugs on demand upon particular stimulations, such as pH, temperature, enzyme presence, etc. [4].

Phototherapy

It is a non-intrusive, affordable, with short-term solution procedure remotely activated for the treatment of diseases. Overall, it is classified into two subcategories, namely photodynamic therapy (PDT) [32,127] and photothermal therapy (PTT) [47,128]. In phototherapy procedures, a phototherapeutic agent is addressed to a specific site that requires treatment for irradiation of light at a particular wavelength. In a PDT approach, photosensitizers (PS) promote non-reversible harms of cells while creating reactive oxygen species by light. As for PTT methods, photothermal (PT) agents absorb light in the near infrared (NIR) spectrum, heat the material, and provoke ablation of cells. 2DQDs have key features as PT agents, including fluorescence properties, photostability, chemical stability, and biocompatibility. Examples of 2DQDs candidates for phototherapy as MoS_2-QDs [117,129], WS_2-QDs [42], nitrogen-doped GQDs functionalized with amino groups [130], as fabricated GQDs [131] as well as sulphur-doped GQDs [132], BPQDs and PEGylated BPQDs [133].

7. Conclusions

The studies and outcomes observed in the field of 2D materials over the last decade has established this field as one of the fastest growing topics in material science. It is known that there are thousands of stable crystalline 2D materials [134–136], so that although much has already been done in this area, there are still opportunities for researchers to produce impactful research in this area. 2D quantum dots (2DQDs) is one of the most important sub-fields of 2D materials' research because of their unique characteristics and potential technological applications.

In this review, we focused on the methods of production (top-down and bottom-up approaches), functionalization routes, and the PL properties of 2DQDs. We have shown that there is a large number of strategies for synthesis and options of characterization techniques suitable for these materials. We showed that because 2DQDs have electronic flexibility, which is determined by geometry and composition, they are excellent platforms for biosensing and bioimaging, and they have been explored for using in such challenging problems, such as in theranostic applications for cancer treatment.

The progress in this area is tremendous and every year more discoveries are made. Hence, 2DQD is an exciting field to work on in its many different aspects from synthesis and characterization to basic science and industrial applications. Additionally, recent discoveries of superconductivity and magnetism in 2D materials broaden the horizon of study of 2DQDs showing that the future in this area is in fact greatly promising.

Author Contributions: Conceptualization, M.C.F.C.; methodology, M.C.F.C. and S.G.E.; data curation, M.C.F.C.; writing—original draft preparation, M.C.F.C.; writing—review and editing M.C.F.C., S.G.E., D.V.A., K.S.N. and A.H.C.N.; funding acquisition, K.S.N. and A.H.C.N. All authors have read and agreed to the published version of the manuscript.

Funding: This work was supported under the Medium-Sized Centre (MSC) grant from the National Research Foundation (NRF) of Singapore, Prime Minister's Office. This research was also supported by the Ministry of Education, Singapore, under its Research Centre of Excellence award to the Institute for Functional Intelligent Materials (I-FIM, project No. EDUNC-33-18-279-V12).

Conflicts of Interest: The authors declare no conflict of interest.

References

1. *ISO/TS 80004-13:2017*; ISO/TC 229 Nanotechnologies. Nanotechnologies—Vocabulary—Part 13: Graphene and Related Two-dimenszional (2D) Materials. ISO: Geneva, Switzerland, 2017.
2. Ekimov, A.I.; Efros, A.L.; Onushchenko, A.A. Quantum size effect in semiconductor microcrystals. *Solid State Commun.* **1985**, *56*, 921–924. [CrossRef]
3. Alhassid, Y. The statistical theory of quantum dots. *Rev. Mod. Phys.* **2000**, *72*, 895–968. [CrossRef]
4. Gidwani, B.; Sahu, V.; Shukla, S.S.; Pandey, R.; Joshi, V.; Jain, V.K.; Vyas, A. Quantum dots: Prospectives, toxicity, advances and applications. *J. Drug Deliv. Sci. Technol.* **2021**, *61*, 102308. [CrossRef]
5. Jameson, D.M.; James, N.G.; Albanesi, J.P. Fluorescence Fluctuation Spectroscopy Approaches to the Study of Receptors in Live Cells. *Methods Enzymol.* **2013**, *519*, 87–113. [PubMed]
6. Vahala, K.J. Optical microcavities. *Nature* **2003**, *424*, 839–846. [CrossRef] [PubMed]
7. Arul, V.; Edison, T.N.J.I.; Lee, Y.R.; Sethuraman, M.G. Biological and catalytic applications of green synthesized fluorescent N-doped carbon dots using Hylocereus undatus. *J. Photochem. Photobiol. B Biol.* **2017**, *168*, 142–148. [CrossRef]
8. Roy, P.; Periasamy, A.P.; Chuang, C.; Liou, Y.-R.; Chen, Y.-F.; Joly, J.; Liang, C.-T.; Chang, H.-T. Plant leaf-derived graphene quantum dots and applications for white LEDs. *New J. Chem.* **2014**, *38*, 4946–4951. [CrossRef]
9. Coe-Sullivan, S.; Liu, W.; Allen, P.; Steckel, J.S. Quantum Dots for LED Downconversion in Display Applications. *ECS J. Solid State Sci. Technol.* **2013**, *2*, R3026–R3030. [CrossRef]
10. Lim, H.; Liu, Y.; Kim, H.Y.; Son, D.I. Facile synthesis and characterization of carbon quantum dots and photovoltaic applications. *Thin Solid Films* **2018**, *660*, 672–677. [CrossRef]
11. Abolghasemi, R.; Rasuli, R.; Alizadeh, M. Microwave-assisted growth of high-quality CdSe quantum dots and its application as a sensitizer in photovoltaic cells. *Mater. Today Commun.* **2020**, *22*, 100827. [CrossRef]
12. Hetsch, F.; Zhao, N.; Kershaw, S.V.; Rogach, A.L. Quantum dot field effect transistors. *Mater. Today* **2013**, *16*, 312–325. [CrossRef]
13. Choi, B.H.; Hwang, S.W.; Kim, I.G.; Shin, H.C.; Kim, Y.; Kim, E.K. Fabrication and room-temperature characterization of a silicon self-assembled quantum-dot transistor. *Appl. Phys. Lett.* **1998**, *73*, 3129–3131. [CrossRef]

14. Wu, G.Y.; Lue, N.-Y.; Chang, L. Graphene quantum dots for valley-based quantum computing: A feasibility study. *Phys. Rev. B* **2011**, *84*, 195463. [CrossRef]
15. Zhu, S.; Zhang, J.; Tang, S.; Qiao, C.; Wang, L.; Wang, H.; Liu, X.; Li, B.; Li, Y.; Yu, W.; et al. Surface chemistry routes to modulate the photoluminescence of graphene quantum dots: From fluorescence mechanism to up-conversion bioimaging applications. *Adv. Funct. Mater.* **2012**, *22*, 4732–4740. [CrossRef]
16. Xu, S.; Li, D.; Wu, P. One-pot, facile, and versatile synthesis of monolayer MoS2 /WS2 quantum dots as bioimaging probes and efficient electrocatalysts for hydrogen evolution reaction. *Adv. Funct. Mater.* **2015**, *25*, 1127–1136. [CrossRef]
17. Liu, Q.; Lu, X.; Li, J.; Yao, X.; Li, J. Direct electrochemistry of glucose oxidase and electrochemical biosensing of glucose on quantum dots/carbon nanotubes electrodes. *Biosens. Bioelectron.* **2007**, *22*, 3203–3209. [CrossRef]
18. Freeman, R.; Gill, R.; Shweky, I.; Kotler, M.; Banin, U.; Willner, I. Biosensing and Probing of Intracellular Metabolic Pathways by NADH-Sensitive Quantum Dots. *Angew. Chem. Int. Ed.* **2009**, *48*, 309–313. [CrossRef]
19. Bera, D.; Qian, L.; Tseng, T.-K.; Holloway, P.H. Quantum Dots and Their Multimodal Applications: A Review. *Materials* **2010**, *3*, 2260–2345. [CrossRef]
20. Dhanabalan, S.C.; Dhanabalan, B.; Ponraj, J.S.; Bao, Q.; Zhang, H. 2D–Materials-Based Quantum Dots: Gateway towards Next-Generation Optical Devices. *Adv. Opt. Mater.* **2017**, *5*, 1700257. [CrossRef]
21. LAI, S.; Chen, M.; Khanin, Y.N.; Novoselov, K.S.; Andreeva, D.V. Enhancement of reduced graphene oxide bolometric photoresponse via addition of graphene quantum dots. *Surf. Rev. Lett.* **2021**, *28*, 2140011. [CrossRef]
22. Xu, Q.; Cai, W.; Li, W.; Sreeprasad, T.S.; He, Z.; Ong, W.-J.; Li, N. Two-dimensional quantum dots: Fundamentals, photoluminescence mechanism and their energy and environmental applications. *Mater. Today Energy* **2018**, *10*, 222–240. [CrossRef]
23. Kittel, C. *Introduction to Solid State Physics*, 8th ed.; Wiley: Hoboken, NJ, USA, 2004; ISBN 978-0-471-41526-8.
24. Chung, I.; Shimizu, K.T.; Bawendi, M.G. Room temperature measurements of the 3D orientation of single CdSe quantum dots using polarization microscopy. *Proc. Natl. Acad. Sci. USA* **2003**, *100*, 405–408. [CrossRef]
25. Cusack, M.A.; Briddon, P.R.; Jaros, M. Electronic structure of InAs/GaAs self-assembled quantum dots. *Phys. Rev. B* **1996**, *54*, R2300–R2303. [CrossRef]
26. Meric, I.; Han, M.Y.; Young, A.F.; Ozyilmaz, B.; Kim, P.; Shepard, K.L. Current saturation in zero-bandgap, top-gated graphene field-effect transistors. *Nat. Nanotechnol.* **2008**, *3*, 654–659. [CrossRef] [PubMed]
27. Schwierz, F. Graphene Transistors: Status, Prospects, and Problems. *Proc. IEEE* **2013**, *101*, 1567–1584. [CrossRef]
28. Ezawa, M. Peculiar band gap structure of graphene nanoribbons. *Phys. Status Solidi* **2007**, *4*, 489–492. [CrossRef]
29. Manikandan, A.; Chen, Y.-Z.; Shen, C.-C.; Sher, C.-W.; Kuo, H.-C.; Chueh, Y.-L. A critical review on two-dimensional quantum dots (2D QDs): From synthesis toward applications in energy and optoelectronics. *Prog. Quantum Electron.* **2019**, *68*, 100226. [CrossRef]
30. Shen, J.; Zhu, Y.; Yang, X.; Li, C. Graphene quantum dots: Emergent nanolights for bioimaging, sensors, catalysis and photovoltaic devices. *Chem. Commun.* **2012**, *48*, 3686. [CrossRef]
31. Wang, X.; Sun, G.; Li, N.; Chen, P. Quantum dots derived from two-dimensional materials and their applications for catalysis and energy. *Chem. Soc. Rev.* **2016**, *45*, 2239–2262. [CrossRef] [PubMed]
32. Xu, Y.; Wang, X.; Zhang, W.L.; Lv, F.; Guo, S. Recent progress in two-dimensional inorganic quantum dots. *Chem. Soc. Rev.* **2018**, *47*, 586–625. [CrossRef] [PubMed]
33. Zhu, H.; Ni, N.; Govindarajan, S.; Ding, X.; Leong, D.T. Phototherapy with layered materials derived quantum dots. *Nanoscale* **2020**, *12*, 43–57. [CrossRef] [PubMed]
34. Fan, L.; Zhu, M.; Lee, X.; Zhang, R.; Wang, K.; Wei, J.; Zhong, M.; Wu, D.; Zhu, H. Direct Synthesis of Graphene Quantum Dots by Chemical Vapor Deposition. *Part. Part. Syst. Charact.* **2013**, *30*, 764–769. [CrossRef]
35. Luo, Y.; Xu, Y.; Li, M.; Sun, L.; Hu, G.; Tang, T.; Wen, J.; Li, X. Tuning the Photoluminescence of Graphene Quantum Dots by Fluorination. *J. Nanomater.* **2017**, *2017*, 9682846. [CrossRef]
36. Kim, S.; Hwang, S.W.; Kim, M.K.; Shin, D.Y.; Shin, D.H.; Kim, C.O.; Yang, S.B.; Park, J.H.; Hwang, E.; Choi, S.H.; et al. Anomalous behaviors of visible luminescence from graphene quantum dots: Interplay between size and shape. *ACS Nano* **2012**, *6*, 8203–8208. [CrossRef] [PubMed]
37. Liu, F.; Jang, M.H.; Ha, H.D.; Kim, J.H.; Cho, Y.H.; Seo, T.S. Facile synthetic method for pristine graphene quantum dots and graphene oxide quantum dots: Origin of blue and green luminescence. *Adv. Mater.* **2013**, *25*, 3657–3662. [CrossRef] [PubMed]
38. Suvarnaphaet, P.; Pechprasarn, S. Graphene-based materials for biosensors: A review. *Sensors* **2017**, *17*, 2161. [CrossRef] [PubMed]
39. Xu, Y.; Yan, L.; Li, X.; Xu, H. Fabrication of transition metal dichalcogenides quantum dots based on femtosecond laser ablation. *Sci. Rep.* **2019**, *9*, 2931. [CrossRef]
40. Lin, L.; Xu, Y.; Zhang, S.; Ross, I.M.; Ong, A.C.M.; Allwood, D.A. Fabrication and luminescence of monolayered boron nitride quantum dots. *Small* **2014**, *10*, 60–65. [CrossRef]
41. Kong, Z.; Hu, W.; Jiao, F.; Zhang, P.; Shen, J.; Cui, B.; Wang, H.; Liang, L. Theoretical Evaluation of DNA Genotoxicity of Graphene Quantum Dots: A Combination of Density Functional Theory and Molecular Dynamics Simulations. *J. Phys. Chem. B* **2020**, *124*, 9335–9342. [CrossRef]
42. Yong, Y.; Cheng, X.; Bao, T.; Zu, M.; Yan, L.; Yin, W.; Ge, C.; Wang, D.; Gu, Z.; Zhao, Y. Tungsten Sulfide Quantum Dots as Multifunctional Nanotheranostics for In Vivo Dual-Modal Image-Guided Photothermal/Radiotherapy Synergistic Therapy. *ACS Nano* **2015**, *9*, 12451–12463. [CrossRef]

43. Shi, M.; Dong, L.; Zheng, S.; Hou, P.; Cai, L.; Zhao, M.; Zhang, X.; Wang, Q.; Li, J.; Xu, K. "Bottom-up" preparation of MoS2 quantum dots for tumor imaging and their in vivo behavior study. *Biochem. Biophys. Res. Commun.* **2019**, *516*, 1090–1096. [CrossRef] [PubMed]
44. Roy, P.; Periasamy, A.P.; Lin, C.-Y.; Her, G.-M.; Chiu, W.-J.; Li, C.-L.; Shu, C.-L.; Huang, C.-C.; Liang, C.-T.; Chang, H.-T. Photoluminescent graphene quantum dots for in vivo imaging of apoptotic cells. *Nanoscale* **2015**, *7*, 2504–2510. [CrossRef] [PubMed]
45. Wang, D.; Chen, J.F.; Dai, L. Recent advances in graphene quantum dots for fluorescence bioimaging from cells through tissues to animals. *Part. Part. Syst. Charact.* **2015**, *32*, 515–523. [CrossRef]
46. Yadav, V.; Roy, S.; Singh, P.; Khan, Z.; Jaiswal, A. 2D MoS2-Based Nanomaterials for Therapeutic, Bioimaging, and Biosensing Applications. *Small* **2019**, *15*, 1803706. [CrossRef]
47. Hu, S.H.; Chen, Y.W.; Hung, W.T.; Chen, I.W.; Chen, S.Y. Quantum-dot-tagged reduced graphene oxide nanocomposites for bright fluorescence bioimaging and photothermal therapy monitored in situ. *Adv. Mater.* **2012**, *24*, 1748–1754. [CrossRef]
48. Du, Y.; Guo, S. Chemically doped fluorescent carbon and graphene quantum dots for bioimaging, sensor, catalytic and photoelectronic applications. *Nanoscale* **2016**, *8*, 2532–2543. [CrossRef]
49. Hatamluyi, B.; Rezayi, M.; Amel Jamehdar, S.; Rizi, K.S.; Mojarrad, M.; Meshkat, Z.; Choobin, H.; Soleimanpour, S.; Boroushaki, M.T. Sensitive and specific clinically diagnosis of SARS-CoV-2 employing a novel biosensor based on boron nitride quantum dots/flower-like gold nanostructures signal amplification. *Biosens. Bioelectron.* **2022**, *207*, 114209. [CrossRef]
50. Chronopoulos, D.D.; Bakandritsos, A.; Pykal, M.; Zbořil, R.; Otyepka, M. Chemistry, properties, and applications of fluorographene. *Appl. Mater. Today* **2017**, *9*, 60–70. [CrossRef] [PubMed]
51. Sun, X.; Lei, Y. Fluorescent carbon dots and their sensing applications. *TrAC Trends Anal. Chem.* **2017**, *89*, 163–180. [CrossRef]
52. Zuo, P.; Lu, X.; Sun, Z.; Guo, Y.; He, H. A review on syntheses, properties, characterization and bioanalytical applications of fluorescent carbon dots. *Microchim. Acta* **2016**, *183*, 519–542. [CrossRef]
53. Fernandes, J.O.; Bernardino, C.A.R.; Braz, B.F.; Mahler, C.F.; Santelli, R.E.; Cincotto, F.H. (Bio)Sensing Materials: Quantum Dots. In *Reference Module in Biomedical Sciences*; Elsevier: Amsterdam, The Netherlands, 2021.
54. Da Costa, M.C.F.; Ribeiro, H.B.; Kessler, F.; de Souza, E.A.T.; Fechine, G.J.M. Micromechanical exfoliation of two-dimensional materials by a polymeric stamp. *Mater. Res. Express* **2016**, *3*, 025303. [CrossRef]
55. Qiu, X.; Bouchiat, V.; Colombet, D.; Ayela, F. Liquid-phase exfoliation of graphite into graphene nanosheets in a hydrocavitating 'lab-on-a-chip'. *RSC Adv.* **2019**, *9*, 3232–3238. [CrossRef] [PubMed]
56. Hernandez, Y.; Nicolosi, V.; Lotya, M.; Blighe, F.M.; Sun, Z.; De, S.; McGovern, I.T.; Holland, B.; Byrne, M.; Gun'Ko, Y.K.; et al. High-yield production of graphene by liquid-phase exfoliation of graphite. *Nat. Nanotechnol.* **2008**, *3*, 563–568. [CrossRef] [PubMed]
57. Zhang, T.; Zhao, H.; Fan, G.; Li, Y.; Li, L.; Quan, X. Electrolytic exfoliation synthesis of boron doped graphene quantum dots: A new luminescent material for electrochemiluminescence detection of oncogene microRNA-20a. *Electrochim. Acta* **2016**, *190*, 1150–1158. [CrossRef]
58. Qiao, W.; Yan, S.; Song, X.; Zhang, X.; He, X.; Zhong, W.; Du, Y. Luminescent monolayer MoS2 quantum dots produced by multi-exfoliation based on lithium intercalation. *Appl. Surf. Sci.* **2015**, *359*, 130–136. [CrossRef]
59. Najafi, L.; Bellani, S.; Martín-García, B.; Oropesa-Nuñez, R.; Del Rio Castillo, A.E.; Prato, M.; Moreels, I.; Bonaccorso, F. Solution-Processed Hybrid Graphene Flake/2H-MoS 2 Quantum Dot Heterostructures for Efficient Electrochemical Hydrogen Evolution. *Chem. Mater.* **2017**, *29*, 5782–5786. [CrossRef]
60. Lin, D.; Su, Z.; Wei, G. Three-dimensional porous reduced graphene oxide decorated with MoS2 quantum dots for electrochemical determination of hydrogen peroxide. *Mater. Today Chem.* **2018**, *7*, 76–83. [CrossRef]
61. Smith, A.M.; Duan, H.; Rhyner, M.N.; Ruan, G.; Nie, S. A systematic examination of surface coatings on the optical and chemical properties of semiconductor quantum dots. *Phys. Chem. Chem. Phys.* **2006**, *8*, 3895. [CrossRef] [PubMed]
62. Gopalakrishnan, D.; Damien, D.; Shaijumon, M.M. MoS 2 Quantum Dot-Interspersed Exfoliated MoS 2 Nanosheets. *ACS Nano* **2014**, *8*, 5297–5303. [CrossRef]
63. Li, B.L.; Chen, L.X.; Zou, H.L.; Lei, J.L.; Luo, H.Q.; Li, N.B. Electrochemically induced Fenton reaction of few-layer MoS 2 nanosheets: Preparation of luminescent quantum dots via a transition of nanoporous morphology. *Nanoscale* **2014**, *6*, 9831–9838. [CrossRef]
64. Cong, S.; Tian, Y.; Li, Q.; Zhao, Z.; Geng, F. Single-Crystalline Tungsten Oxide Quantum Dots for Fast Pseudocapacitor and Electrochromic Applications. *Adv. Mater.* **2014**, *26*, 4260–4267. [CrossRef] [PubMed]
65. Wang, J.; Li, G.; Li, L. Synthesis Strategies about 2D Materials. In *Two-Dimensional Materials—Synthesis, Characterization and Potential Applications*; InTech: Vienna, Austria, 2016.
66. Li, R.; Liu, Y.; Li, Z.; Shen, J.; Yang, Y.; Cui, X.; Yang, G. Bottom-Up Fabrication of Single-Layered Nitrogen-Doped Graphene Quantum Dots through Intermolecular Carbonization Arrayed in a 2D Plane. *Chem. A Eur. J.* **2016**, *22*, 272–278. [CrossRef] [PubMed]
67. Liu, C.; Zhang, P.; Tian, F.; Li, W.; Li, F.; Liu, W. One-step synthesis of surface passivated carbon nanodots by microwave assisted pyrolysis for enhanced multicolor photoluminescence and bioimaging. *J. Mater. Chem.* **2011**, *21*, 13163. [CrossRef]
68. Liu, J.-J.; Zhang, X.-L.; Cong, Z.-X.; Chen, Z.-T.; Yang, H.-H.; Chen, G.-N. Glutathione-functionalized graphene quantum dots as selective fluorescent probes for phosphate-containing metabolites. *Nanoscale* **2013**, *5*, 1810. [CrossRef]

69. Kagan, C.R.; Bassett, L.C.; Murray, C.B.; Thompson, S.M. Colloidal Quantum Dots as Platforms for Quantum Information Science. *Chem. Rev.* **2021**, *121*, 3186–3233. [CrossRef]
70. Lin, H.; Wang, C.; Wu, J.; Xu, Z.; Huang, Y.; Zhang, C. Colloidal synthesis of MoS 2 quantum dots: Size-dependent tunable photoluminescence and bioimaging. *New J. Chem.* **2015**, *39*, 8492–8497. [CrossRef]
71. Jung, W.; Lee, S.; Yoo, D.; Jeong, S.; Miró, P.; Kuc, A.; Heine, T.; Cheon, J. Colloidal Synthesis of Single-Layer MSe 2 (M = Mo, W) Nanosheets via Anisotropic Solution-Phase Growth Approach. *J. Am. Chem. Soc.* **2015**, *137*, 7266–7269. [CrossRef]
72. Musselman, K.P.; Ibrahim, K.H.; Yavuz, M. Research Update: Beyond graphene—Synthesis of functionalized quantum dots of 2D materials and their applications. *APL Mater.* **2018**, *6*, 120701. [CrossRef]
73. Liu, M.; Xu, Y.; Wang, Y.; Chen, X.; Ji, X.; Niu, F.; Song, Z.; Liu, J. Boron Nitride Quantum Dots with Solvent-Regulated Blue/Green Photoluminescence and Electrochemiluminescent Behavior for Versatile Applications. *Adv. Opt. Mater.* **2017**, *5*, 1600661. [CrossRef]
74. Lu, Y.-C.; Chen, J.; Wang, A.-J.; Bao, N.; Feng, J.-J.; Wang, W.; Shao, L. Facile synthesis of oxygen and sulfur co-doped graphitic carbon nitride fluorescent quantum dots and their application for mercury(II) detection and bioimaging. *J. Mater. Chem. C* **2015**, *3*, 73–78. [CrossRef]
75. Qu, D.; Zheng, M.; Du, P.; Zhou, Y.; Zhang, L.; Li, D.; Tan, H.; Zhao, Z.; Xie, Z.; Sun, Z. Highly luminescent S, N co-doped graphene quantum dots with broad visible absorption bands for visible light photocatalysts. *Nanoscale* **2013**, *5*, 12272. [CrossRef] [PubMed]
76. Geng, P.; Wang, L.; Du, M.; Bai, Y.; Li, W.; Liu, Y.; Chen, S.; Braunstein, P.; Xu, Q.; Pang, H. MIL-96-Al for Li–S Batteries: Shape or Size? *Adv. Mater.* **2022**, *34*, 2107836. [CrossRef] [PubMed]
77. Li, W.; Guo, X.; Geng, P.; Du, M.; Jing, Q.; Chen, X.; Zhang, G.; Li, H.; Xu, Q.; Braunstein, P.; et al. Rational Design and General Synthesis of Multimetallic Metal–Organic Framework Nano-Octahedra for Enhanced Li–S Battery. *Adv. Mater.* **2021**, *33*, 2105163. [CrossRef] [PubMed]
78. Zheng, X.T.; Than, A.; Ananthanaraya, A.; Kim, D.-H.; Chen, P. Graphene Quantum Dots as Universal Fluorophores and Their Use in Revealing Regulated Trafficking of Insulin Receptors in Adipocytes. *ACS Nano* **2013**, *7*, 6278–6286. [CrossRef] [PubMed]
79. Ou, L.; Song, B.; Liang, H.; Liu, J.; Feng, X.; Deng, B.; Sun, T.; Shao, L. Toxicity of graphene-family nanoparticles: A general review of the origins and mechanisms. *Part. Fibre Toxicol.* **2016**, *13*, 57. [CrossRef]
80. Cross, D.; Burmester, J.K. Gene Therapy for Cancer Treatment: Past, Present and Future. *Clin. Med. Res.* **2006**, *4*, 218–227. [CrossRef]
81. Chong, Y.; Ge, C.; Yang, Z.; Garate, J.A.; Gu, Z.; Weber, J.K.; Liu, J.; Zhou, R. Reduced Cytotoxicity of Graphene Nanosheets Mediated by Blood-Protein Coating. *ACS Nano* **2015**, *9*, 5713–5724. [CrossRef]
82. Akhavan, O.; Ghaderi, E.; Emamy, H.; Akhavan, F. Genotoxicity of graphene nanoribbons in human mesenchymal stem cells. *Carbon N. Y.* **2013**, *54*, 419–431. [CrossRef]
83. Lv, M.; Zhang, Y.; Liang, L.; Wei, M.; Hu, W.; Li, X.; Huang, Q. Effect of graphene oxide on undifferentiated and retinoic acid-differentiated SH-SY5Y cells line. *Nanoscale* **2012**, *4*, 3861. [CrossRef]
84. Zhang, X.; Hu, W.; Li, J.; Tao, L.; Wei, Y. A comparative study of cellular uptake and cytotoxicity of multi-walled carbon nanotubes, graphene oxide, and nanodiamond. *Toxicol. Res.* **2012**, *1*, 62–68. [CrossRef]
85. Wang, D.; Zhu, L.; Chen, J.-F.; Dai, L. Can graphene quantum dots cause DNA damage in cells? *Nanoscale* **2015**, *7*, 9894–9901. [CrossRef] [PubMed]
86. Cai, K.-B.; Huang, H.-Y.; Hsieh, M.-L.; Chen, P.-W.; Chiang, S.-E.; Chang, S.H.; Shen, J.-L.; Liu, W.-R.; Yuan, C.-T. Two-Dimensional Self-Assembly of Boric Acid-Functionalized Graphene Quantum Dots: Tunable and Superior Optical Properties for Efficient Eco-Friendly Luminescent Solar Concentrators. *ACS Nano* **2022**, *16*, 3994–4003. [CrossRef] [PubMed]
87. Shayeganfar, F.; Rahimi Tabar, M.R.; Simchi, A.; Beheshtian, J. Effects of functionalization and side defects on single-photon emission in boron nitride quantum dots. *Phys. Rev. B* **2017**, *96*, 165307. [CrossRef]
88. Scotognella, F.; Kriegel, I.; Sassolini, S. Covalent functionalized black phosphorus quantum dots. *Opt. Mater.* **2018**, *75*, 521–524. [CrossRef]
89. Raheman AR, S.; Wilson, H.M.; Momin, B.M.; Annapure, U.S.; Jha, N. CdSe quantum dots modified thiol functionalized g-C3N4: Intimate interfacial charge transfer between 0D/2D nanostructure for visible light H2 evolution. *Renew. Energy* **2020**, *158*, 431–443. [CrossRef]
90. Stokes, G.G. On the change of refrangibility of light. No. II. *Abstr. Pap. Commun. R. Soc. Lond.* **1854**, *6*, 333–335. [CrossRef]
91. Crosby, G.A.; Demas, J.N. Measurement of photoluminescence quantum yields. Review. *J. Phys. Chem.* **1971**, *75*, 991–1024. [CrossRef]
92. Wen, J.; Xu, Y.; Li, H.; Lu, A.; Sun, S. Recent applications of carbon nanomaterials in fluorescence biosensing and bioimaging. *Chem. Commun.* **2015**, *51*, 11346–11358. [CrossRef]
93. Fan, Z.; Li, S.; Yuan, F.; Fan, L. Fluorescent graphene quantum dots for biosensing and bioimaging. *RSC Adv.* **2015**, *5*, 19773–19789. [CrossRef]
94. Biju, V.; Ishikawa, M. Photoluminescence of CdSe Quantum Dots: Shifting, Enhancement and Blinking. In *Molecular Nano Dynamics*; Wiley-VCH Verlag GmbH & Co. KGaA: Weinheim, Germany, 2009; pp. 293–314.
95. *ISO 13095:2014*; Surface Chemical Analysis—Atomic Force Microscopy—Procedure for in Situ Characterization on AFM Probe Shank Profile Used for Nanostructure Measurement. Standards: Etobicoke, ON, Canada, 2014.

96. Kumar, S.; Ojha, A.K.; Ahmed, B.; Kumar, A.; Das, J.; Materny, A. Tunable (violet to green) emission by high-yield graphene quantum dots and exploiting its unique properties towards sun-light-driven photocatalysis and supercapacitor electrode materials. *Mater. Today Commun.* **2017**, *11*, 76–86. [CrossRef]
97. Sarkar, S.; Gandla, D.; Venkatesh, Y.; Bangal, P.R.; Ghosh, S.; Yang, Y.; Misra, S. Graphene quantum dots from graphite by liquid exfoliation showing excitation-independent emission, fluorescence upconversion and delayed fluorescence. *Phys. Chem. Chem. Phys.* **2016**, *18*, 21278–21287. [CrossRef] [PubMed]
98. Costa, M.C.F.; Marangoni, V.S.; Ng, P.R.; Nguyen, H.T.L.; Carvalho, A.; Castro Neto, A.H. Accelerated Synthesis of Graphene Oxide from Graphene. *Nanomaterials* **2021**, *11*, 551. [CrossRef] [PubMed]
99. Carvalho, A.; Costa, M.C.F.; Marangoni, V.S.; Ng, P.R.; Nguyen, T.L.H.; Castro Neto, A.H. The Degree of Oxidation of Graphene Oxide. *Nanomaterials* **2021**, *11*, 560. [CrossRef] [PubMed]
100. Fadeel, B.; Fornara, A.; Toprak, M.S.; Bhattacharya, K. Keeping it real: The importance of material characterization in nanotoxicology. *Biochem. Biophys. Res. Commun.* **2015**, *468*, 498–503. [CrossRef] [PubMed]
101. Verma, P.; Kuwahara, Y.; Mori, K.; Raja, R.; Yamashita, H. New insights in establishing the structure-property relations of novel plasmonic nanostructures for clean energy applications. *EnergyChem* **2022**, *4*, 100070. [CrossRef]
102. Sharifi, S.; Behzadi, S.; Laurent, S.; Forrest, M.L.; Stroeve, P.; Mahmoudi, M. Toxicity of nanomaterials. *Chem. Soc. Rev.* **2012**, *41*, 2323–2343. [CrossRef]
103. Clark, L.C.; Lyons, C. Electrode systems for continuous monitoring in cardiovascular surgery. *Ann. N. Y. Acad. Sci.* **2006**, *102*, 29–45. [CrossRef]
104. Hu, X.; Zhou, Q. Health and Ecosystem Risks of Graphene. *Chem. Rev.* **2013**, *113*, 3815–3835. [CrossRef]
105. Colvin, V.L. The potential environmental impact of engineered nanomaterials. *Nat. Biotechnol.* **2003**, *21*, 1166–1170. [CrossRef]
106. Zhou, K.; Zhang, Y.; Xia, Z.; Wei, W. As-prepared MoS 2 quantum dot as a facile fluorescent probe for long-term tracing of live cells. *Nanotechnology* **2016**, *27*, 275101. [CrossRef]
107. Duan, J.; Yu, Y.; Li, Y.; Yu, Y.; Li, Y.; Huang, P.; Zhou, X.; Peng, S.; Sun, Z. Developmental toxicity of CdTe QDs in zebrafish embryos and larvae. *J. Nanopart. Res.* **2013**, *15*, 1700. [CrossRef]
108. Zhang, W.; Lin, K.; Miao, Y.; Dong, Q.; Huang, C.; Wang, H.; Guo, M.; Cui, X. Toxicity assessment of zebrafish following exposure to CdTe QDs. *J. Hazard. Mater.* **2012**, *213–214*, 413–420. [CrossRef]
109. Wang, Z.G.; Zhou, R.; Jiang, D.; Song, J.E.; Xu, Q.; Si, J.; Chen, Y.P.; Zhou, X.; Gan, L.; Li, J.Z.; et al. Toxicity of graphene quantum dots in zebrafish embryo. *Biomed. Environ. Sci.* **2015**, *28*, 341–351. [CrossRef] [PubMed]
110. Appel, J.H.; Li, D.O.; Podlevsky, J.D.; Debnath, A.; Green, A.A.; Wang, Q.H.; Chae, J. Low Cytotoxicity and Genotoxicity of Two-Dimensional MoS 2 and WS 2. *ACS Biomater. Sci. Eng.* **2016**, *2*, 361–367. [CrossRef]
111. Medintz, I.L.; Uyeda, H.T.; Goldman, E.R.; Mattoussi, H. Quantum dot bioconjugates for imaging, labelling and sensing. *Nat. Mater.* **2005**, *4*, 435–446. [CrossRef]
112. Kawamura, A.; Miyata, T. Biosensors. *Biomater. Nanoarchitect.* **2016**, 157–176, Chapter 4.2. [CrossRef]
113. Michelmore, A. *Thin Film Growth on Biomaterial Surfaces*; Elsevier Ltd.: Amsterdam, The Netherlands, 2016; ISBN 9781782424536.
114. Qian, Z.S.; Shan, X.Y.; Chai, L.J.; Ma, J.J.; Chen, J.R.; Feng, H. A universal fluorescence sensing strategy based on biocompatible graphene quantum dots and graphene oxide for the detection of DNA. *Nanoscale* **2014**, *6*, 5671–5674. [CrossRef] [PubMed]
115. Ju, J.; Zhang, R.; He, S.; Chen, W. Nitrogen-doped graphene quantum dots-based fluorescent probe for the sensitive turn-on detection of glutathione and its cellular imaging. *RSC Adv.* **2014**, *4*, 52583–52589. [CrossRef]
116. Wu, S.; Kong, X.J.; Cen, Y.; Yuan, J.; Yu, R.Q.; Chu, X. Fabrication of a LRET-based upconverting hybrid nanocomposite for turn-on sensing of H2O2 and glucose. *Nanoscale* **2016**, *8*, 8939–8946. [CrossRef]
117. Shi, J.; Lyu, J.; Tian, F.; Yang, M. A fluorescence turn-on biosensor based on graphene quantum dots (GQDs) and molybdenum disulfide (MoS2) nanosheets for epithelial cell adhesion molecule (EpCAM) detection. *Biosens. Bioelectron.* **2017**, *93*, 182–188. [CrossRef]
118. Liu, Y.; Zhang, J.; Shen, Y.; Yan, J.; Hou, Z.; Mao, C.; Zhao, W. MoS 2 quantum dots featured fluorescent biosensor for multiple detection of cancer. *RSC Adv.* **2017**, *7*, 54638–54643. [CrossRef]
119. Sreejith, S.; Joshi, H.; Zhao, Y. Graphene-Based Materials in Biosensing, Bioimaging, and Therapeutics. In *Graphene-Based Materials in Health and Environment*; Springer: Cham, Switzerland, 2016; pp. 35–61.
120. Dong, H.; Tang, S.; Hao, Y.; Yu, H.; Dai, W.; Zhao, G.; Cao, Y.; Lu, H.; Zhang, X.; Ju, H. Fluorescent MoS 2 Quantum Dots: Ultrasonic Preparation, Up-Conversion and Down-Conversion Bioimaging, and Photodynamic Therapy. *ACS Appl. Mater. Interfaces* **2016**, *8*, 3107–3114. [CrossRef]
121. Xue, Q.; Zhang, H.; Zhu, M.; Wang, Z.; Pei, Z.; Huang, Y.; Huang, Y.; Song, X.; Zeng, H.; Zhi, C. Hydrothermal synthesis of blue-fluorescent monolayer BN and BCNO quantum dots for bio-imaging probes. *RSC Adv.* **2016**, *6*, 79090–79094. [CrossRef]
122. Li, Y.; Liu, Z.; Hou, Y.; Yang, G.; Fei, X.; Zhao, H.; Guo, Y.; Su, C.; Wang, Z.; Zhong, H.; et al. Multifunctional Nanoplatform Based on Black Phosphorus Quantum Dots for Bioimaging and Photodynamic/Photothermal Synergistic Cancer Therapy. *ACS Appl. Mater. Interfaces* **2017**, *9*, 25098–25106. [CrossRef] [PubMed]
123. Fan, Z.; Li, Y.; Li, X.; Fan, L.; Zhou, S.; Fang, D.; Yang, S. Surrounding media sensitive photoluminescence of boron-doped graphene quantum dots for highly fluorescent dyed crystals, chemical sensing and bioimaging. *Carbon N. Y.* **2014**, *70*, 149–156. [CrossRef]

124. Dolmans, D.E.J.G.J.; Fukumura, D.; Jain, R.K. Photodynamic therapy for cancer. *Nat. Rev. Cancer* **2003**, *3*, 380–387. [CrossRef] [PubMed]
125. Liu, H.; Chen, D.; Li, L.; Liu, T.; Tan, L.; Wu, X.; Tang, F. Multifunctional Gold Nanoshells on Silica Nanorattles: A Platform for the Combination of Photothermal Therapy and Chemotherapy with Low Systemic Toxicity. *Angew. Chem. Int. Ed.* **2011**, *50*, 891–895. [CrossRef]
126. Ding, X.; Peng, F.; Zhou, J.; Gong, W.; Slaven, G.; Loh, K.P.; Lim, C.T.; Leong, D.T. Defect engineered bioactive transition metals dichalcogenides quantum dots. *Nat. Commun.* **2019**, *10*, 41. [CrossRef]
127. Kuo, W.-S.; Shao, Y.-T.; Huang, K.-S.; Chou, T.-M.; Yang, C.-H. Antimicrobial Amino-Functionalized Nitrogen-Doped Graphene Quantum Dots for Eliminating Multidrug-Resistant Species in Dual-Modality Photodynamic Therapy and Bioimaging under Two-Photon Excitation. *ACS Appl. Mater. Interfaces* **2018**, *10*, 14438–14446. [CrossRef] [PubMed]
128. Ristic, B.Z.; Milenkovic, M.M.; Dakic, I.R.; Todorovic-Markovic, B.M.; Milosavljevic, M.S.; Budimir, M.D.; Paunovic, V.G.; Dramicanin, M.D.; Markovic, Z.M.; Trajkovic, V.S. Photodynamic antibacterial effect of graphene quantum dots. *Biomaterials* **2014**, *35*, 4428–4435. [CrossRef]
129. Kholikov, K.; Ilhom, S.; Sajjad, M.; Smith, M.E.; Monroe, J.D.; San, O.; Er, A.O. Improved singlet oxygen generation and antimicrobial activity of sulphur-doped graphene quantum dots coupled with methylene blue for photodynamic therapy applications. *Photodiagn. Photodyn. Ther.* **2018**, *24*, 7–14. [CrossRef] [PubMed]
130. Guo, T.; Wu, Y.; Lin, Y.; Xu, X.; Lian, H.; Huang, G.; Liu, J.-Z.; Wu, X.; Yang, H.-H. Black Phosphorus Quantum Dots with Renal Clearance Property for Efficient Photodynamic Therapy. *Small* **2018**, *14*, 1702815. [CrossRef]
131. Mas-Ballesté, R.; Gómez-Navarro, C.; Gómez-Herrero, J.; Zamora, F. 2D materials: To graphene and beyond. *Nanoscale* **2011**, *3*, 20–30. [CrossRef] [PubMed]
132. Miró, P.; Audiffred, M.; Heine, T. An atlas of two-dimensional materials. *Chem. Soc. Rev.* **2014**, *43*, 6537–6554. [CrossRef] [PubMed]
133. Novoselov, K.S.; Mishchenko, A.; Carvalho, A.; Castro Neto, A.H. 2D materials and van der Waals heterostructures. *Science* **2016**, *353*, aac9439. [CrossRef] [PubMed]
134. Guzman, D.M.; Alyahyaei, H.M.; Jishi, R.A. Superconductivity in graphene-lithium. *2D Mater.* **2014**, *1*, 021005. [CrossRef]
135. Thiel, L.; Wang, Z.; Tschudin, M.A.; Rohner, D.; Gutiérrez-Lezama, I.; Ubrig, N.; Gibertini, M.; Giannini, E.; Morpurgo, A.F.; Maletinsky, P. Probing magnetism in 2D materials at the nanoscale with single-spin microscopy. *Science* **2019**, *364*, 973–976. [CrossRef] [PubMed]
136. Sethulakshmi, N.; Mishra, A.; Ajayan, P.M.; Kawazoe, Y.; Roy, A.K.; Singh, A.K.; Tiwary, C.S. Magnetism in two-dimensional materials beyond graphene. *Mater. Today* **2019**, *27*, 107–122. [CrossRef]